Patent Office
Canberra

I, KIM MARSHALL, MANAGER EXAMINATION SUPPORT AND SALES, hereby certify that the annexed is a true copy of the Provisional specification in connection with Application No. PO 7549 for a patent by LUDWIG INSTITUTE FOR CANCER RESEARCH, THE UNIVERSITY OF QUEENSLAND, THE QUEENSLAND INSTITUTE OF MEDICAL RESEARCH and THE LEUKAEMIA FOUNDATION OF QUEENSLAND filed on 25 June 1997.

I further certify that the annexed specification is not, as yet, open to public inspection.

WITNESS my hand this Twenty-fourth
day of July 1998

KIM MARSHALL
MANAGER EXAMINATION SUPPORT AND
SALES

AUSTRALIA

Patents Act 1990

PROVISIONAL SPECIFICATION

Applicant(s): LUDWIG INSTITUTE OF MEDICAL RESEARCH

THE QUEENSLAND INSTITUTE OF MEDICAL RESEARCH

THE UNIVERSITY OF QUEENSLAND

THE LEUKAEMIA FOUNDATION OF QUEENSLAND

Invention Title: RECEPTOR-LIGAND SYSTEM AND ASSAY THEREFOR
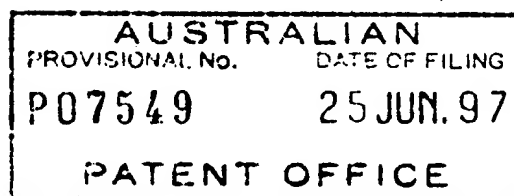
The invention is described in the following statement:

RECEPTOR-LIGAND SYSTEM AND ASSAY THEREFOR

This invention relates to the Eph receptor tyrosine kinase family and to ligands corresponding to the receptor tyrosine kinases. In particular, the invention relates to the receptor Hek, and its corresponding ligand LERK7. The invention provides an assay system whereby the normal function of the expression products of genes encoding Hek and LERK7 can be assessed, and further provides a means of determining the binding and the receptor dimerization domains of the Hek protein. Because of the highly conserved nature of the receptor tyrosine kinases of the Eph family, the methods of the invention are applicable to other members of this family. Hek and other Eph receptor tyrosine kinases are closely involved in embryonic development of the brain, and Hek and other receptors (Eph, Eck, Erk) are associated with leukaemias and solid tumours, and may have a role in metastasis.

BACKGROUND OF THE INVENTION

Increasing interest in the understanding of the molecular basis of tissue modeling and patterning processes in vertebrate development has led to the identification of protein families which direct cell movement in embryogenesis (reviewed by Bonhoeffer and Sanes, 1995)). Apart from members of the fibroblast growth factor (FGF) and transforming growth factor beta (TGFβ) families, which are involved in mesoderm induction and patterning (Green and Smith, 1991), proteins of the netrin, semaphorin and collapsin families are thought to control axon guidance and neural pathfinding (Kennedy and Tessier-Lavigne, 1995; Måller et al, 1996).

Such growth factors and their cell surface receptors, as well as many other types of receptor-ligand pairs, have

characteristic mechanisms for transducing the ligand-receptor binding effect into intracellular changes. One major receptor type is the receptor protein-tyrosine kinase receptor family, in which the receptors have intracellular

5 kinase domains which are activated in response to ligand stimulation, resulting in autophosphorylation of tyrosine residues in the receptor. The phosphorylated tyrosines in turn bind to and activate signaling molecules, commencing a signaling cascade inside the cell. Over fourteen distinct

10 sub-families of receptor protein-tyrosine kinases are known, and of these the largest group is the "Eph" subfamily, which until comparatively recently were "orphan" receptors for which no ligand had been identified. However, the Eph family ligands are now known to represent a family of glycosyl

15 phosphatidylinositol (GPI) -linked or transmembrane molecules.

Among the receptor tyrosine kinases (RTK) implicated in the regulation of developmental patterning events (Pawson and Bernstein, 1990), members of the Eph-like RTKs have been

20 linked to neurogenesis (Müller *et al*, 1996; Tessier-Lavigne, 1995; Pandey *et al*, 1995; Nieto, 1996) initially due to their spatially-restricted expression patterns during the development of the vertebrate nervous system (reviewed by Friedman and O'Leary, 1996). The characterisation of the

25 expression patterns and functional studies of Eph receptors has, in several cases confirmed significant roles for Eph signaling in axon guidance, in particular during the development of the retino-tectal projection map (Cheng and Flanagan, 1994; Cheng *et al*, 1995; Drescher, 1995; Winslow,

30 1995; Tessier-Lavigne, 1995; Brennan *et al*, 1997).

Overexpression of some family members including Hek, EPH, ERK and ECK in tumour-derived cell lines, tumour specimens and transfected cells implicates these receptors in

oncogenesis (Hirai *et al*, 1989; Boyd *et al*, 1992; Maru *et al*, 1990; Andres *et al*, 1994).

Hek was identified on the cell surface of a pre-B acute lymphoblastic leukemia cell line, LK63, using the IIIA4
5   monoclonal antibody (Mab) (Boyd *et al*, 1992). Immunofluorescence studies with IIIA4 revealed expression of Hek in blood samples from patients with acute leukemia, but not in normal adult tissues or blood cells (Boyd *et al*, 1992; Wicks *et al*, 1992). In embryos, the expression patterns of
10   the murine and chicken Hek homologues MEK 4 and CEK 4, and their recently identified ligands ELF1 (12) and RAGS (13), respectively, suggest a role in the development of the retinotectal projection map. We have also isolated a soluble Hek ligand from human placenta conditioned medium using a
15   biosensor-based affinity detection approach (Lackmann *et al*, 1995). The Hek ligand was identified by sequence homology as a soluble form of AL-1 (Winslow *et al,* 1995), a member of the ligands for EPH Related Kinases (LERKs) family (Bohme *et al*, 1996; Cerreti *et al*, 1996), and for consistency with other
20   members will be referred to as LERK 7. This family of transmembrane or membrane-associated proteins were isolated as potential ligands for EPH-like RTKs through their interactions with recombinant EPH receptor family exodomains (Winslow *et al*, 1994; Beckmann *et al*, 1996; Shao *et al*, 1995;
25   Brambilla *et al*, 1995).

Extremely high interspecies sequence similarities of the known Eph family members suggests that these receptors have evolutionarily conserved functions, but little is known about the actual protein structures or about the
30   structure/function relationships between Eph-like receptors and their ligands. Eph RTKs are typified by their exodomain, consisting of an N-terminal cysteine-rich region, the outer portion of which has been described as Ig-like, followed by two fibronectin III regions (Pandey *et al*, 1995; Tuzi and

Gullick, 1994; Henkemeyer, 1994). Extensive cross-reactivity of Eph receptor/ligand interactions has been observed with divalent receptor (ligand) fusion proteins containing the Fc domain of human IgG 1 (Beckmann, 1994; Davis *et al*, 1994;

5 Pandey *et al*, 1994; Cerretti *et al*, 1995; Pandey *et al*, 1995; Brambilla, 1995). All of the known ligands exist as membrane-associated forms, and dependence of receptor activation on membrane bound or oligomerised ligands (Winslow *et al*, 1995; Davis *et al*, 1994) was reported for most members

10 of the Eph-like receptor and ligand families.

The apparent receptor/ligand promiscuity of various receptors and ligands monitored with receptor or ligand Fc-fusion constructs suggested that the Eph receptors could be separated into two redundant sub-classes, based on affinity

15 for transmembrane or GPI-linked ligands respectively. Together with their overlapping expression patterns, this led to a model in which promiscuous interactions within these subclasses mediates formation of spatial boundaries and patterning events during development (Gale *et al*, 1996).

20 This reported redundancy is at odds with several studies which demonstrate specialised functions of the homologous RTKs MEK4/CEK4/RTK2 and their corresponding ligands ELF1/RAGS/zEphL4 during the development of the retinotectal projection map in mouse, chicken and zebrafish (Cheng *et al*,

25 1995; Drescher *et al*, 1995; Nakamoto *et al*, 1996; Brennan *et al*, 1997).

We have now identified the preferred high-affinity ligand for Hek, have identified the ligand-binding domain of the Hek protein, and have detected a putative receptor

30 dimerisation interface. We have also developed a sensitive assay which enables us to examine the function of the Hek protein, modifications thereof and of the ligand to assay for agonists and antagonists of the ligand, and to monitor downstream events following ligand binding. Because of the

role in Eph receptor tyrosine kinases in cell movement during neural development, agonists of ligands for Eph proteins and their receptors are useful in the study of neural tube defects. Because of the role of Hek and other Eph kinases in a variety of cancer conditions and in metastasis, inhibitors of the function of Hek and other Eph kinases, such as antagonists to the ligand binding or to the dimerisation domain have uses as anticancer and/or antimetastatic agents.

SUMMARY OF THE INVENTION

In one aspect, the invention provides a ligand-binding domain of a receptor protein kinase of the Eph family, comprising the cysteine-rich domain encoded by exon III of the Hek gene.

Preferably the ligand-binding domain additionally comprises the protein encoded by exons I and II of the eph gene.

Even more preferably, the ligand binding domain comprises at least one disulphide bond involving cysteine residues corresponding to the following conserved cysteines in Hek:

Cys_{51} - Cys_{169}

Cys_{247} or $_{349}$ - Cys_{169}

Cys_{296} - Cys_{312}

Cys_{353} - Cys_{358}

In one preferred embodiment the Eph ligand binding domain is labelled with FLAG™ peptide.

In a particularly preferred embodiment, the Eph receptor tyrosine kinase is Hek.

In a second aspect, the invention provides a nucleic acid encoding a ligand binding domain of an Eph receptor tyrosine kinase as described above. More preferably the nucleic acid is a cDNA.

In a third aspect of the invention provides the specific monovalent ligand for the receptor Hek.

In a fourth aspect, the invention provides a method of assay of the intactness of a gene transcript encoding the
5   ligand binding domain of an Eph receptor tyrosine kinase, comprising the step of transcribing the gene to mRNA, introducing the mRNA into a zebrafish embryo at the one-cell, two-cell, or four-cell stage, and detecting defects in early embryogenesis in the zebrafish embryo.

10   In a fifth aspect the invention provides a method of assay for the intactness of a gene transcript encoding the ligand for the receptor Hek. Preferably the intactness of the transcript of the first seven exons is assayed.

Preferably the mRNA is introduced into the embryo by
15   microinjection into the yolk cell immediately under the blastoderm. Preferably a syndrome comprising defects involving reduced dorsal axis height from the yolk cell, disorganised anterior neuraxis, and disorganised somite boundaries is detected. More preferably this syndrome of
20   defects is detected in at least 50% of embryos subjected to the test.

Injection of mRNA encoding the soluble ligand LERK7-FLAG™ causes identical effects, whereas co-injection of receptor and ligand mRNA achieves a partial rescue of the
25   phenotype, demonstrating the specificity of the receptor/ligand mediated effects.

In a sixth aspect, the invention provides an alternative method of identifying the site of functional effects of interaction between an Eph receptor tyrosine
30   kinase and its specific ligand, comprising the steps of injecting zebrafish embryos with mRNA encoding the Eph protein, and subjecting the embryos to *in situ* hybridisation with probes to *Hlx-1, Paxb, Krox20* and *MyoD*, and detecting

patterns of *in situ* hybridisation consistent with ectopic, misplaced or absent gene expression.

Preferably the Eph receptor tyrosine kinase is Hek, and the ligand is LERK7. Preferably the assay is used to identify events occurring during embryogenesis.

In a preferred embodiment of the three aspects of the assay method, the Eph protein tyrosine kinase is Hek and the ligand is LERK7. In one particularly preferred embodiment, the gene encoding the Eph protein has the ligand binding domain of exon 3 deleted.

In a seventh aspect, the invention provides a method of analysis of interaction of an Eph protein tyrosine kinase and its corresponding ligand, comprising the step of binding monovalent Eph protein tyrosine kinase to a sensor chip, and measuring the ability of a ligand of putative ligand to bind to the sensor chip, or binding a ligand or putative ligand to a sensor chip, and measuring the binding of an Eph protein tyrosine kinase to the immobilised ligand. Preferably the Eph protein tyrosine kinase is Hek, and the ligand is LERK7. This system may also be used to test candidate compounds for their activity as agonists or antagonists of Eph protein-ligand binding.

Hek is associated with pre-B cell leukaemia and with other leukaemias. Other Eph receptors are associated with solid tumours such as melanoma and cancers of the colon, liver, lung, breast and prostate. Eph receptors are considered to play a role in metastasis, possibly because of its role in cell migration and tissue structure. It is therefore considered that inhibitors of Hek function, for example antagonists of ligand binding or of the Hek dimerisation domain, are potentially useful as anticancer or antimetastatic agents. The assays provided by the invention are useful in identifying compounds which have such antagonist activity. Similarly the assays of the invention

are useful for identification of agonists or antagonists of LERK7.

BRIEF DESCRIPTION OF THE FIGURES

5   Figure 1 shows the genomic organisation of the extracellular region of EPH-like RTK genes and the interaction between sHek-derived subdomains and BIAcore™ sensorchip-immobilised LERK7.

          cDNAs according to the exon structure A) of sHek
10   depicted in Table 1 and Figure 1 were isolated by PCR and transfected into CHO cells as described in Methods. The exons are illustrated in B as differently shaded bars; ☐ , exon 1+2, ☐ , exon 3, ■ , exon 4, ▨ , exon 5, ▧ , exon 6+7. The isolation of exons belonging to Hek, SEK1, BSK and ESK
15   genes is described herein. #Exon VII from the MEK4 gene was reported in Sajjadi *et al* (1991). *The genomic structure of CEK5 is described in Connor and Pasquale. ⊢—⊣ represents 1kb; ---, clone size not determined.

          D)   sHek subdomain proteins at increasing
20   concentrations (15.6 - 500 nM) were injected onto LERK7-derivatised sensor chips and the association rate constants, (■) derived from BIAcore™ raw data using the BIA evaluation software as described in Methods.

          E)   The kinetic rate constants were then used to
25   estimate apparent dissociation constants according to $K_D = k_d/k_a$. The mean and standard deviation from estimates at five different concentrations are shown (■). In addition, equilibrium responses were used to estimate the apparent equilibrium dissociation constants (☐).

30   F)   Samples containing 40 nM LERK 7 and 10 nM - 10 μM of a synthetic peptide according to the sHek sequence encoded by exons 1 and 2 (Δ), 10nM - 1μM sHek IV(☐), or 10nM-1μM sHek I (O) were injected onto a sHek-derivatised sensor chip. The residual responses are illustrated as

percentage fraction of the total response in the absence of competitor.

Figure 2 shows a schematic comparison of native LERK7 with FLAG™ and Fc fusion constructs.

5   In each case the precursor protein is depicted with an arrow leading to the final processed form. The original precursor protein is processed to remove the signal sequence and the hydrophobic glycophosphatidyl inositol linkage sequence (cleavage site indicated by arrow head) yielding the

10   final GPI-linked form (Figure 2A). The LERK7-FLAG™ is engineered to stop before ·the hydrophobic tail and the native N-terminal signal sequence is replaced with the IL3 signal peptide and the FLAG™ epitope (Figure 2B). Figure 2C illustrates the LERK7-Fc construct where the hydrophobic tail

15   of the native sequence is replaced by the Fc and hinge regions of human IgG1. After processing this yields the disulphide linked homodimer (Bohme et al, 1996).

Figure 3 shows a comparison of the binding of LERK-Fc fusion proteins to sensor chip-immobilised Hek.   Samples

20   (50µl) of purified fusion proteins between the human Fc domain and LERKs 1, 2, 3, 4, 5 and 7 at 10µg/ml in BIAcore™ running buffer were applied onto a sHek-derivatised sensor chip.   The responses recorded 20s after completion of the injection phase (■), relative BIAcore™ response units, RU)

25   are compared to the response of an equal amount of human Fc domain used as a control in this experiment.

Figure 4 shows binding curves for the interaction of monovalent LERK-FLAG™ fusion proteins with immobilised sHek.

Homogeneous preparations of CHO cell-derived LERK 3-

30   FLAG™ (panel A) or LERK 7-FLAG™ (panel B) at increasing concentrations (8.22, 16.44, 32.88, 65.75, 131.5, 263, 526 nM LERK3-FLAG™, 1.25, 2.5, 5, 10, 20, 40, 80 nM LERK7-FLAG™) were injected across a sHek-derivatised sensor surface and BIAcore™ data for the association and dissociation phases

were used to estimate corresponding kinetic rate constants on the basis of a one-to-one interaction model. (panel C) Free sHek was estimated in samples of increasing sHek with a constant LERK 7-FLAG™ concentration at equilibrium and used

5   to calculate the equilibrium dissociation constant K_D by Scatchard analysis.

Figure 5 illustrates characterisation of bivalent ligand binding by generation of ternary sHek/LERK-FLAG™/M2-MAb complexes *in situ*.

10   Solutions (5µg/ml) of purified LERK 7-FLAG™ (panels A, B) or LERK 3-FLAG™ (panels C, D) with (sensorgrams e, f) or without addition (sensorgram c) of cross-linking M2-anti-FLAG™ MAb (5µg/ml) were injected across a sHek-derivatised sensor surface (↓1) followed by an subsequent injection (↓2)

15   of buffer (sensorgrams c, e), M2 MAb (5µg/ml, sensorgrams d) or FLAG™ peptide (25 µg/ml, sensorgrams f). For comparison, injections of buffer (↓1) followed (↓2) by M2 MAb or FLAG™ peptide (sensorgrams a and b, respectively) were performed in parallel experiments.

20   Figure 6 illustrates the induction of Hek phosphorylation in LK63 cells by LERK7-FLAG™. The membrane of a Western blot probed with PY20 anti-phosphotyrosine antibody (panel A) was stripped and analysed with rabbit anti-Hek antibody (panel B). Lane 1 - FLAG™-LERK 7/M2

25   antibody complexes, Lane 2 - FLAG™-LERK 3/M2 antibody complexes, Lane 3 - FLAG™-LERK 7, Lane 4 - FLAG™-LERK 3 and in Lane 5 control medium alone.

Figure 7 shows the effect of ectopic expression of the human Hek receptor extracellular domain and of soluble

30   LERK 7 on the development of zebrafish embryos.

Zebrafish embryos were injected with 10 pg of either sHek I-VII RNA or sLERK7 RNA and 5 pg marker mRNA during the first two cleavage divisions and raised at 28°C. Embryos are photographed from a lateral perspective in a- c, with dorsal

to the right and from a dorsal perspective in d-f, with anterior up in each frame.

(a)   a non-injected zebrafish embryo at 12 hpf showing normally developed otic vesicle, forebrain (open arrow head) and tail-butt (closed arrow head) and revealing a normal dorsal height from the yolk surface (H).

(b)   a zebrafish embryo at 12 hpf after microinjection with 10 ng sHek I-VII RNA displaying strong developmental defects in the mid- and hind brain, poorly developed otic vesicle (open arrow head) reduced height of the dorsal axis from the yolk surface (H) and absence of somitic grooves and tail-butt (closed arrow head).

(c)   a zebrafish embryo at 12 hpf after microinjection with 10 ng sLERK 7 RNA displaying an identical phenotype to the sHek I-VII RNA injected specimen.

(d)   dorsal view of the non-injected embryo illustrated in a), revealing well-developed somitic grooves, 'lining up in register' along the midline.

(e,f)   Dorsal views of embryos shown in b,c showing poorly developed somites.

Figure 8 shows the analysis of sHek- and sLERK 7-mediated developmental effects by *in-situ* hybridisation. Embryos were injected with 10 pg of either sHek I-VII RNA or sLERK 7 RNA, allowed to develop for 12 to 13 hpf and fixed for in situ hybridisation with *pax-b*, *hlx-1*, *krox20* and *myoD* DIG-labeled riboprobes.   Embryos are photographed from a dorsal perspective with anterior to the top and posterior to the bottom of each frame; a, c, e, antero-dorsal view; b, d, f, posterio-dorsal view.

(a,b)   Uninjected embryo at 12 hpf showing normal expression of *hlx-1*in the ventral forebrain, *pax-b* in the midbrain , *krox20* in rhombomeres 3 and 5 of the hindbrain and *myoD* in the paraxial mesoderm.

(c,d)   sHek I-VII RNA (10 pg) injected embryo at 12 hpf showing *pax-b* and *krox20* expressing cells in the mid and hindbrain extensively displaced from the midline. *myoD* expressing cells of the paraxial mesoderm displaced from the midline are visible posterior to the brain. An intact *hlx-1* stripe is present anteriorly.

(e,f)   sLERK 7 RNA (10 pg) injected embryo at 12 hpf demonstrating a phenotype which is almost identical to that of the sHek I-VII RNA injected embryo shown in c,d.

Figure 9 shows that the ectopic expression of the Hek receptor construct sHek IV-VII, missing the ligand binding domain, does not affect the development of zebrafish embryos.

a)   Detection of endogenous sHek I-VII and sHek IV-VII in zebrafish embryos by Western blot and BIAcore analysis. Samples of lysis buffer or zebrafish lysates (10 embryos/0.1 ml) containing 25, 20, 5, 2.5 ng of sHek I-VII and sHek IV-VII were immunoprecipitated with anti-FLAG™ MAb (M2) agarose and analysed by Western blot. Zebrafish embryos injected with sHek I-VII RNA or sHek IV-VII RNA were lysed after 5h or 10 h and analysed in parallel lanes of the gel. Specific detection of FLAG™ epitope-containing proteins corresponding to the expected molecular weight for sHek I-VII and sHek VI-VII in embryos at 5 and 10 hpf demonstrates that the recombinant fusion proteins were present in embryos throughout the period of development analysed here. Parallel BIAcore analysis of whole embryo lysates with sensorchips derivatised with native conformation-specific anti-Hek MAb (Boyd, 1992; Lackmann *et al*, 1996) detects the intact receptor exodomain at an apparent concentration of 120 to 240 ng per embryo (5 to 10 hpf, respectively, data not shown).

(b-d) Zebrafish embryos were injected with 10 pg of either sHek I-RNA or sHek IX- RNA and 5 pg marker mRNA during the first two cleavage divisions and raised at 28°C. Embryos

are photographed from a lateral perspective in b, c, d, with dorsal to the right and anterior up in each frame.

(b)   a zebrafish embryo at 12 hpf after microinjection with 10 ng sHek I-VII RNA displaying a strong example of the syndrome. Severe anterior defects, a reduced height of the dorsal axis from the yolk surface and absence of somitic grooves are visible.

(c)   15hpf embryo after injection with 10 pg sHek IV–VII RNA. The morphology of these embryos is indistinguishable from that of non-injected control embryos (Figure 7a).

(d)   The same embryo viewed under epifluorescence illumination to detect translation of coinjected E-GFP marker mRNA demonstrating widespread and high level expression.

(e)   Uninjected embryo at 12 hpf showing normal expression of *hlx-1*in the ventral forebrain, *pax-b* in the midbrain , *krox20* in rhombomeres 3 and 5 of the hindbrain and *myoD* in the paraxial mesoderm.

(f)   sHek I-VII RNA (10 pg) injected embryo at 12 hpf showing *pax-b* and *krox20* expressing cells in the mid and hindbrain extensively displaced from the midline. *myoD* expressing cells of the paraxial mesoderm displaced from the midline are visible posterior to the brain. An intact *hlx-1* stripe is present anteriorly.

(g)   sHek IV-VII RNA (10 pg) injected embryo at 12 hpf demonstrating normal expression of *hlx-1, pax-b , krox20* and *myoD*. By comparison with (e) the embryo in (g) is rotated ~30° anteriorly.

Figure 10 shows the dose response of developmental defects to injected RNA.

a)   Batches of embryos, injected with indicated amounts of sHek I-VII RNA (closed bars), sLERK 7-RNA (open bars) or a combination of both (cross-lined bars) and a constant amount of E-GFP mRNA (5 pg) were allowed to grow for

12 to 13 hpf before fixation and hybridisation with *pax-b*,
hlx-1, *krox20* and *myoD* DIG-labeled riboprobes. Embryos were
analysed under a dissecting microscope and scored for
dirupted patterns of gene expression. Non-injected control

5   embryos were scored after an identical development period and
identical handling, in the same maner as the injected embryos
to control for defects due to the genetic background of
particular parents in our strain. In these experiments, none
of the control embryos revealed any develomental defects.

10   b)   Batches of embryos, injected with indicated
amomounts sHek I-VII RNA (closed bars), sHek VI-VII RNA (open
bars) or non-injected control embryos (cross-lined bars) were
analysed as described in a).

15 DETAILED DESCRIPTION OF THE INVENTION
We have now shown that monovalent ligand constructs
interact with Hek with markedly different affinities, with
LERK7/AL-1 being 50-fold more avid than LERK3. This suggests
that these receptors do not show true redundancy, but rather

20 use varying affinity for different, and possibly overlapping,
ligand gradients for fine control of cell movement within the
developing organism.
In this specification we describe studies of the exon
structure of extracellular portion of the Hek gene and

25 related RTK to demonstrate a consensus structure for all
these genes. Deletion mutants of the Hek exodomain were
constructed based on these data and expressed protein
obtained. With the elucidation of the Hek gene structure as
a starting point we exploited the specific interaction

30 between Hek and LERK7 in a biosensor-based strategy to
identify the N-terminal, exon III-encoded cysteine-rich
subdomain as the ligand binding domain.
These receptor exodomain constructs were analysed
functionally in a dominant-negative approach by micro-

injecting mRNA encoding either the full-length receptor exodomain (sHek-I-VII-RNA) or the soluble ligand (sLERK7-RNA) or a deletion construct of the receptor, in which the coding sequence for the ligand binding domain (sHek-IV-VII-RNA) was
5   absent, into zebrafish embryos. Whereas injection of sHekI-VII-RNA and of sLERK7-RNA had severe, dose-dependent effects on the development of the fish embryos, a phenotype comparable to non-injected control embryos was observed at moderate concentrations of injected sHek-IV-VII-RNA and
10 expression of comparable amounts of the exogenous protein.

In addition to severely impaired mid and hindbrain development, prominent effects on axis and somite formation were observed early during development (12-14 h post fertilisation, hpf), in accord with the early expression
15 patterns of the putative zebrafish Hek homologue RTK2 (N. Holder, personal communication) starting at 80-90% epiboly (9 hpf) as reported previously by Xu et al, 1994). The defects are consistent with a failure of lateral cells to move towards the midline as part of the cell movements enacted
20 during gastrulation. Furthermore, our results raise the possibility of an endogenous signal mediated by a LERK7 homologue and required by lateral cells for migration towards the midline.

Our data demonstrate a pivotal role of Hek /RTK2
25 during early vertebrate embryogenesis, and indicate that a defined ligand/receptor interaction has critical functions at progressive developmental stages.

Abbreviations used herein are as follows:
    DIG   digoxigenin
30 ECL   enhanced chemiluminescence
    E-GFP   glycophosphatidyl inositol
    FLAG™   refers to the amino acid sequence DYKDDDDK
    GPI   to be provided
    Mab   monoclonal antibody

PAGE   polyacrylamide electrophoresis
PBS   phosphate buffered saline
PVDF   polivinylidene difluoride
RP-HPLC   reverse phase high performance ligand
5   chromatography
RTK   receptor tyrosine kinase
RU   relative response units
SE   size exclusion
sHek   soluble Hek extracellular domain
10

     The invention will now be described in detail by way
of reference only to the following non-limiting methods and
experimental examples.

15 <u>Methods</u>
Isolation and mapping of Hek genomic clones
     The Hek cDNA probes used to screen the human genomic
libary were PCR fragments amplified from plasmids containing
full length Hek cDNA.   The primers used were:
20   probe A (spans 74bp to 1161bp as described by Wicks
et al, 1992)
     GTAGGAATTCCTCTCACTGCCCTCTGC and
     GTAGGGATCCGGCCTCCTGTTCCAG,
Probe B (1053bp to 1124 bp)
25   GTAGGAATTCCATGG CTTGTACCCGAC and
     GTAGGGATCCCATAATGCTTGCTTCTC,
probe C (2bp to 186bp)
     ATGG ATGGTAACTTCTCCAG and TCATTGGAAGGCTGCGGAAT, and
probe D (spans 909bp to 1404bp)
30   GTAGTCTAGACAAGCTTGTCGACCAGGTTT and
     GTAGTCTAGATCAAGCCTGATTAGTTG TGATGC.

     The mouse genomic library was screened with a MEK4
fragment cut from a plasmid subcloned with MEK4 cDNA (kindly

provided by Dr E Pasquale, University of California at San Diego). The cDNA fragment spans 582bp to 899bp of the MEK4 sequence (Sajjadi *et al*, 1991).

    The genomic libraries used were human in 1 FIX II
5 vector, (Stratagene Cloning Systems, La Jolla) and mouse in 1 FIX II vector (Stratagene) and 1 DASH II vector (kindly provided by F.Köntgen, Walter and Eliza Hall Institute for Medical Research, Melbourne). Approximately 10^6 plaques from each library were plated, replica nylon membrane filters
10 (Bio-Rad Laboratories, New York) were prehybridized at 42°C in 50% formamide, 10x Denhardt's solution, 0.05M Tris-Cl pH 7.5, 1.0M NaCl, 2.24mM tetra-sodium pyrophosphate, 1% SDS, 10% dextran sulfate and 0.1mg/ml sheared, heat-denatured herring sperm DNA, and the filters hybridized at 42°C for 16
15 hours. Washes were performed at 68°C in 0.1 x SSC, 0.1% SDS for 1 hour and in 0.1 x SSC, 0.5% SDS for a further 30 min. Positive clones were identified by autoradiography, purified by subsequent screenings and isolated using standard methodology (Sambrook *et al*, 1989). Exon-intron boundaries
20 were determined by a combination of direct DNA sequencing, PCR, restriction analyses, and Southern blotting. Direct DNA sequencing of the genomic 1 phages and subcloned plasmid was performed using the ABI 373 DNA sequencer (Applied Biosystems, Melbourne, Australia). Sequencing and PCR
25 primers used to characterize the Hek gene from human genomic clones were based on the Hek cDNA sequence (Wicks *et al*, 1992).

    The exons found within the mouse genomic clones were amplified by PCR using degenerate primers specific to EPH-
30 like RTKs,
GTAGGCATGCAAGGAGA C(AC)TT(CT)AACC and
CC(AG)ATGGGNACCAGCCA(CT)TC.
The PCR products were then directly sequenced as described above using the degenerate primers.

Production of sHek and sHek sub-domains in CHO cells

　　　　sHek and N-terminally FLAG™-tagged sHek proteins were prepared from transfected Chinese Hamster ovary (CHO) cell

5　supernatants as previously described (Lackmann *et al*, 1996). Deletion mutants of sHek were prepared by PCR using oligos based on the exon boundaries.　Hek III and IV were constructed using a 5' oligonucleotide based on the N terminal sequence of the mature protein (Boyd *et al*, 1992)

10　with a　5' XbaI site　　　(GTAGTCTAGAGAACTGATTCCGCAGCCTTCCAA) and 3' oligonucleotides based on sequences spanning exon 4

　　　　(GTAGTCTAGATCATGGAGGTCGGGTACAAGC)
and 3

　　　　(GTAGTCTAGATCAAGCTTGGCACATAAAACCTC)

15　respectively, followed by a stop codon and an XbaI site. Construct IX used a 5' oligo designed to span the 5' end of exon 4　with a 5' XbaI site

　　　　(GTAGTCTAGACAAGCTTGTCGACCAGGTTTC)
and a 3' oligonucleotide based on the C-terminus of the

20　exodomain with a stop codon and flanking XbaI site

　　　　(GTAGTCTAGATCATTGGCTACTTTCACC AGAG).

　　　　In each case the PCR products were cloned into the IL3 signal-FLAG™-pEFBOS vector as previously described (Lackmann, 1996).　DNA was electroporated into CHO cells

25　(Lackmann, 1996), and high producer clones were selected by "dot blot" screening of culture supernatants on PVDF membranes, and the expected size of the recombinant proteins confirmed by SDS-PAGE and Western blot analysis　using M2 anti-FLAG™ MAb and rabbit anti-mouse AP-tagged MAb for

30　detection by enhanced chemiluminescence (ECL, Amersham).

　　　　Deletion mutants were purified on M2 anti-FLAG™ affinity columns and eluted with FLAG™ peptide according to the manufacturer's instructions.　Homogenous preparations (> 95% by SDS-PAGE and silver staining) were obtained by anion

exchange (Mono Q, 5x50 mm, Pharmacia, Uppsala, Sweden) and size exclusion chromatography (Superose 12, 10 x 300 mm, Pharmacia, Uppsala, Sweden). The identity and concentration of the purified sHek proteins in the final preparations were

5   confirmed by N-terminal amino acid sequence analysis and amino acid analysis and, where applicable, their native conformation confirmed on the BIAcore™ as previously described (Lackmann, 1996).

10 *Production of LERK-3 and LERK7 (AL-1) expression constructs*
          The 5' LERK7 oligonucleotide
(GTAGTCTAGACAGGACCCGGGCTCCAAGGC) was based on the N-terminal amino acid sequence (QDPGSKA) of the mature protein, with a 5' tag sequence and XbaI site preceding the coding

15 nucleotides. The PCR reaction was performed using an aliquot of a placental cDNA library (kindly provided by Dr Tracy Wilson, Walter & Eliza Hall Institute) and Taq EXTEND (Boehringer-Mannheim). A 490 bp product was detected on a 1.4% TAE/agarose gel. This was excised and the DNA purified

20 using Geneclean II (BIO101). The PCR product and the IL3 sig-FLAG™-pEFBOS vector (Nicola *et al*, 1996) were digested with XbaI and the vector treated with calf intestinal alkaline phosphatase to prevent re-ligation. After ligation correctly oriented clones were detected and verified by

25 automated DNA sequencing (Model 373, Applied Biosystems, Inc. automated DNA sequencer).

Transfection of cells with LERK 3 and LERK 7 DNA
          Purified LERK7-pEFBOS DNA was transfected into CHO

30 cells. Briefly, 2×10^7 cells were suspended in 500µl of PBS and 10µg of LERK-pEFBOS DNA and 1µg of pSV2neo DNA added. After mixing and transfer to a 0.4 cm electroporation cuvette (BioRad), the cells were electroporated at 270V and 960µFD and the cells centrifuged through an FCS underlayer.

Transfectant clones were selected in medium containing
600µg/ml of G418. Individual clones were isolated and
samples (5µl) of CHO cell supernatants from confluent
cultures were dotted onto a nitrocellulose membrane, air-died
5   and re-hydrated in blocking buffer (5% skim milk powder/0.1%
Tween 20 in PBS) prior to incubation with M2 anti-FLAG™
antibody at 1:1000 dilution. After washing the blot was
incubated with horse radish peroxidase-conjugated rabbit
anti-mouse Ig antibody (1:1000, Dako) in blocking buffer and
10   following further washes developed with the ECL detection
system (Amersham)

Positives clones, indicated by signals above
background, were retested by analysis on SDS-PAGE (12%) and
Western blots prepared and probed as described above to
15   confirm the presence of FLAG™ proteins of the expected
molecular size.

Production of FLAG™-tagged LERK7 /AL-1

LERK7/AL-1 containing an N-terminal FLAG™ peptide was
20   purified from transfected CHO cell supernatants by affinity
extraction on anti-FLAG™ MAb agarose according to the
manufacturer's protocol (IBI Kodak, New Haven CT) followed by
MonoQ (Pharmacia Biotech) ion exchange chromatography in 20
mM Tris, pH 8.5/ 0.02% Tween 20 at 1 ml/min using a linear,
25   40 min gradient from 0 - 600 mM NaCl and SE-HPLC
(Superose 12, 10/30, Pharmacia Biotech) in 20 mM Tris,
pH 7.4/150 mM NaCl/0.02% Tween 20 at 0.25 ml/min. The
homogeneity, concentration and identity of the purified
proteins were confirmed by RP-HPLC, SDS-PAGE, amino acid
30   analysis and N-terminal amino acid sequence analysis as
described (Lackmann *et al*, 1996; Simpson *et al*, 1986).

Synthesis of sHek-derived peptides

The peptide according to the amino acid sequence encompassing residues Glu_1 to Gly_{31} (Hek 1-31) of sHek was assembled by solid-phase peptide synthesis according to
5   standard protocols, purified by RP-HPLC and its mass confirmed by mass spectrometry.

Analysis of the interaction between sHek constructs and LERK7/AL-1
10   The binding of various sHek constructs and derived peptides was analysed on the BIAcore™ optical biosensor (Pharmacia Biosensor, Sweden) using purified sHek or LERK7-FLAG™ derivatised CM 5 sensor chips and the interaction kinetics determined. The immobilisation of sHek onto the
15   sensor chip surface was performed essentially as described by Lackmann *et al*, 1996. LERK7-FLAG™ (47 µg/ml in 20 mM Na-acetate, pH 4.5) was coupled at 5 µl/min onto N-hydroxysuccinimide (NHS, 0.05 M)/N-hydroxysuccinimide-N-ethyl-N′-(diethylaminopropyl)-carbodiimide (EDC, 0.2 M) -
20   activated sensor chips (45 µl, 2µl/min) to yield an increase in the response level of 2500 - 3000 response units (RU).

The interaction kinetics of LERK-binding to immobilised sHek was analysed from raw data of the BIAcore™ sensorgrams suitable for analysis using linear and non-linear
25   kinetic models included in the BIAevaluation software (Biosensor, 1995). All results recorded in this report were within the typical dynamic ranges of BIAcore™ measurements (k_a, 10^3 - 10^6 $M^{-1}s^{-1}$; k_d, 10^{-5} - $10^{-1}s^{-1}$, BIAcore™ catalogue 1996/97) and the BIAevaluation software. Single component
30   kinetics was derived from:

dissociation   : $R = R_0.e^{-k_d(t-t_0)}$ (equation 1)

association   : $R = R_0/k_s.(1-e^{-k_s(t-t_0)}$ (equation 2)

or

$$: R = R_{eq}(1-e^{-k_s(t-t_0)}); \quad k_s = k_aC+k_d \quad \text{(equation 3)}$$

where R_0 is the response at time t_0, R_{eq} the steady state response level (not neccessarily reached in the sensorgram) and C the molar concentration of the analyte. The two component dissociation was derived from:

$$R = R_1 e^{(-k_{d1} \cdot (t-t_0)} + (R_0-R_1) e^{-k_{d2} \cdot (t-t_0)}$$
(equation 4).

Apparent affinities of LERKs 3, 4, 5, 7 were also derived from equilibrium responses according to:
$$R_{eq}/C = K_A R_{max} - K_A R_{eq} \quad \text{(equation 5)},$$

where R_{eq} and R_{max} are the equilibrium and maximum response levels, respectively. In addition to the analysis of ligand binding to sensor chip-immobilised sHek, the interaction between LERK-3 and LERK-7 with sHek was studied in solution. A constant ligand concentration was incubated with increasing concentrations of the soluble receptor. The free ligand concentration (F_{LERK}), estimated from the BIAcore™ response of a known LERK sample was used to calculate the concentration of bound receptor ($[B_{Hek}]$) or ligand ($[B_{LERK}]$), and free sHek (F_{Hek}) using the initial receptor concentration (T_{Hek}) and assuming in this case a single site interaction : $[F_{Hek}] = [T_{Hek}]-[B_{Hek} \cdot B_{LERK}]$, where $[B_{Hek} \cdot B_{LERK}] = [B_{Hek}] = [B_{LERK}]$.
Thus the dissociation constant, K_D, was estimated from:

$$K_D = \frac{[F_{Hek}] \cdot [F_{LERK}]}{[B_{Hek} \cdot B_{LERK}]} = [F_{Hek}] \frac{[F_{LERK}]}{[B_{LERK}]}$$
(equation 6)

according to Ward *et al*, 1995, and Scatchard transformation yielded:

$$5 \qquad \frac{[B_{LERK}]}{[F_{LERK}]} = \frac{1}{K_D} [F_{Hek}]$$

The effect of sHek-derived peptides on the interaction of Hek with LERK7 was tested by incubation of a
10 constant concentration of the ligand with increasing amounts of peptide prior to analysis on a sHek-derivatised sensor chip. The affinity surface was regenerated between subsequent injections of samples with a 35 µl-injection of 50 mM 1,2-diethylamine/0.1% Triton X100, followed by two
15 washes with BIAcore running buffer (Hepes buffered saline/0.005% Tween 20).

Fish care and embryo collection

Wild type zebrafish were obtained from St. Kilda
20 Aquarium (Melbourne) and were kept essentially as described by Westerfield *et al* (1995). Embryos were obtained by natural spawning between a small number (4-10) of male and female fish. Embryos were removed from the spawning tanks within 20 minutes of fertilisation, cleaned in system water,
25 and transferred to the injection apparatus.

RNA synthesis

Constructs equivalent to full length soluble Hek
(sHek I-VII) and sHek IV-VIII and sLERK7 were generated by
30 PCR from the cDNA constructs described above. In each case the 5' oligonucleotide was based on the IL-3 signal sequence and the 3' oligonucleotides were as above except that BglII sites were used to clone the PCR products into the pSP64TK vector. mRNA from the sHek and sLERK7 constructs and a
35 control E-GFP cDNA construct were transcribed *in vitro* using

the mMessage mMaker kit (Ambion, Texas) and resuspended in water at a concentration of $0.1mg.mL^{-1}$ in small aliquots. Integrity of the RNA was checked by denaturing gel electrophoresis of the resulting products. Immediately prior to injection, aliquots of sHek I-VII, sHek IV-VII or sLERK7 were thawed and mixed with water and E-GFP mRNA to a final concentration such that either 100pg, 10pg, or 1pg of the receptor mRNA, and 5pg of the E-GFP mRNA were delivered to each embryo.

Microinjection

Approximately 600pl of RNA, dissolved in water at the desired concentrations, was injected into one-, two- or four-cell embryos under a Wild stereo microscope using Leitz micromanipulators (Leitz, Wetzlar, Germany) and compressed nitrogen. The needle was positioned under the blastoderm in the region of cytoplasmic streaming. Successful injection was judged in the first instance by a visible bolus of fluid in the embryo. Uptake and translation of mRNA by the embryo was measured by including 5pg mRNA encoding E-GFP as a marker in each injection. Injection of over 100pg E-GFP mRNA per embryo does not cause developmental defects. The translation of the injected Hek mRNA was measured at intervals during embryogenesis by Western blotting. Ten embryos per time point were lysed in embryo lysis buffer (25 mM Tris-HCl, pH 7.4, 0.5M NaCl, 1% Triton X-100), immunoprecipitated with anti-FLAG™ M2 monoclonal antibody coupled agarose, subjected to SDS-PAGE, transferred to PVDF-Plus membranes and Western blotted with soluble M2 antibody. Detection of antigen was visualised with ECL. Protein levels were quantitated by densitometric comparison with Hek-FLAG™ mass standards run in the same gel.

Analysis of developmental defects

The effects on embryonic growth of each of the injected mRNAs were measured in two ways. Firstly, embryos were allowed to grow for twelve to thirteen hours after
5   fertilisation [five to eight somite stage (Kimmel *et al*, 1995)], their gross morphology was noted under a dissecting microscope, and the perturbation of early gene expression patterns was assayed by *in situ* hybridisation using digoxigen-labeled RNA probes. Secondly, embryos were scored
10   as defective if a typical pattern of gene expression was disrupted, *ie.* misshapen, missing or ectopic.

Example 1   <u>Genomic Structure of the Extracellular Region</u>
                         <u>of the Hek Gene</u>
15   A human genomic library was screened with the sHek cDNA probes described above, and positive clones were characterized by restriction mapping and Southern blotting using exon-specific oligonucleotides derived from the Hek cDNA sequence. Exons were identified by sequencing subcloned
20   genomic fragments, or by directly sequencing the phage clones with Hek oligonucleotides. A clone containing exon II was not obtained, and its sequence was inferred from the 3' and 5' junctions of exon I and exon III respectively. Sequences for intron-exon splice junctions were matched using the 'GT-
25   AG' rule (Mount, 1982), and the results, summarised in Table 1 and Figure 1a show that the extracellular region consists of seven exons interrupted by six introns.

Table 1

Exon	Splice Acceptor			Splice Donor				
I* (88bp)	ccagcaac	M ATG	D GAT	C TGT	S TCC	N AAT	E GAA	G gtaagcca
II# (65bp)		V TC	N AAT	L CTA	S TCA	H CAT	G GGG	
III (661bp)	ttcttcag	W TGG	E GAA	E GAG	M ATG	C TGC	Q CAA	G gtaagagc
IV (156bp)	gtttgtag	A CT	C TGT	R CGA	A GCT	C TGT	T ACC	C gtgagtag
V (336bp)	ctttgcag	R GA	P CCT	P CCA	N AAT	Q CAG	A GCT	G gtgagtac
VI (126bp)	ctttacag	A CT	P CCA	S TCA	Y TAT	E GAA	K AAG	gtggggaa
VII (163bp)	cctcaaag	Q CAG	E GAA	Q CAA	S AGT	P CCA	D GAC	T gtatgtat

Exon boundaries were determined by sequencing non-
5   overlapping λFIX II clones, and are shown for the
extracellular domains of the Hek gene.

This sequence is the flanking region of the start
methionine, as deduced fromt he published cDNA sequence [REF]

10   #   A λ clone for this exon was not isolated; the exon
boundaries are deduced from the boundaries of the adjacent
exons.

The parallel isolation and analysis of clones from a
15   mouse genomic library containing exons II and III of SEK1,
exon III of BSK, and exon IV of ESK indicates that this
arrangement is a general feature of the EPH-like RTK. The
results are illustrated in Figure 1, and together with
reports on the structure of chicken CEK5 gene (Connor and

Pasquale, 1995) and splice variants of other EPH-like RTKs (Sajjadi *et al*, 1991; Maisonpierre *et al*, 1993) suggest that exon structure is highly conserved within the EPH subfamily.

Exon I contains all of the 5' untranslated sequence
5   and the first 88bp of the coding sequence which including the signal peptide, and together with exon II encodes the first 31 residues of the mature protein (Wicks *et al*, 1994).

Exon III contains ten of the twenty conserved cysteine residues characteristic of this subfamily. Although
10 previous reports have described this cysteine-rich domain of EPH-like kinases as being immunoglobulin-like, we found no significant homology between exon III and any other protein domains in the database using the ALIGN sequence alignment program. It has been suggested that the carboxy terminus of
15 exon III is similiar to an EGF-like repeat as it contains the consensus sequence motif CnCxCxxGYnC (Table 2, Connor and Pasquale, 1995). Although the genomic organization is not typical of a repeat (see below), we believe that exon III arose from a fusion or shuffling of exons which once encoded
20 an EGF-like module.

Database analysis of the exon IV sequence showed matches with EGF repeat regions in other proteins. Moreover, the six conserved cysteine residues follow a CnCnCnCXCnC pattern, which is characteristic of an EGF-like repeat (Table
25 2) found within the EGF precursor gene (Bell *et al*, 1986). EGF-like repeats are usually encoded by a discrete exon, as noted in the genomic organization of EGF precursor protein, LDL receptor, and human factor IX (Anson *et al*, 1984; Sudhof *et al*, 1985; Bell *et al*, 1986).

30 The exon-intron borders of the two fibronectin domains correlate exactly with the borders predicted by analysis of the amino acid sequence. The first fibronectin type III repeat is encoded by a single exon, which also contains the remaining four conserved cytsteine residues

found within EPH-like RTKs. Exon VI and exon VII encode the second fibronectin repeat. The genomic organization of the fibronectin type III repeats is typical of the type III homology units found within the fibronectin gene and other
5   proteins containing fibronectin repeats (Oldberg and Ruoslahti, 1986; Giger *et al*, 1995). The fibronectin type III units are encoded by either a single exon or by two exons; however, the units which are spliced out in various protein isoforms are usually those encoded by a single exon
10   (Oldberg and Ruoslahti, 1986). This is also observed with transcripts of EPH family members which lack the first fibronectin repeat (Maisonpierre *et al*, 1993).

Example 2   Assignment of the Disulphide bonds in sHek
15   The structural importance of disulphide bonds for the architecture of a protein or protein domain is undisputed. Although the connectivities of 8 of the conserved cysteines in exons 3 and 4 are inferred from the respective domain structures, as shown in Table 2, assignment of remaining
20   disulphide bridges in exon 3 and an experimental confirmation of the predicted Cys-Cys bonding pattern were critical requirements for a reliable expression of conformationally stable receptor subdomains.

Table 2

EGF-LIKE REPEATS

```
                                              C - (12) - C S C N A G Y - (6) - C     Hek
                                              C - (12) - C L C N A G H - (6) - C     SEK1
 5                                            C - (12) - C H C E P G Y - (8) - C     EPH    Exon III
                                              C - (12) - C M C R P G Y - (8) - C     CEK5
                                              C - (12) - C T C K A G Y - (7) - C     ELK

10   C - (13) - C A K C - (13) - C - (12) - C R C E N N Y - (11) - C     Hek
     C - (13) - C A K C - (13) - C - (12) - C T C D R G F - (11) - C     SEK1
     C - (13) - C L T C - (13) - C - (12) - C T C E S G H - (11) - C     EPH    Exon IV
     C - (13) - C V H C - (13) - C - (12) - C V C R N G Y - (11) - C     CEK5
     C - (13) - C S H C - (13) - C - (12) - C T C R T G Y - (11) - C     ELK

15   C - (7) - C S Q L C - (9) - C - (12) - C D C F P G Y - (8) - C     PREPRO-EGF
     C - (6) - C E H I C - (8) - C - (12) - C S C R E G F - (8) - C     PREPRO-EGF
     C - (6) - C S H V C - (8) - C - (12) - C L C P D G F - (7) - C     LDL Receptor
     C - (6) - C D Q F C - (8) - C - (12) - C S C A R G Y - (8) - C     Factor X
20   C - (6) - C E Q F C - (9) - C - (12) - C S C T E G Y - (8) - C     Factor IX
     C - (6) - C A H Y C - (8) - C - (12) - C S C A P G Y - (8) - C     Protein C
     C (n) C (n) C (n) C x C xx G Y/F (n) C     CONSENSUS
```

In a strategy adopted from Hodder *et al* (1996), we analysed reduced and non-reduced tryptic maps of the minimally-glycosylated sHek by analytical RP-HPLC, to rapidly identify disulphide-containing fragments as absorbance peaks unique to the RP-HPLC profile of the non-reduced tryptic digest. Automated N-terminal amino acid sequence analysis and mass-spectrometry of these peptides enabled identification of the disulphides within the native receptor exodomain.

Assignment of the following peptides was confirmed:

Cys_{51} - Cys_{169}	(C1-C4)
Cys_{247} or $_{349}$ - Cys_{169}	(C8/9-C10)
Cys_{296} - Cys_{312}	(C15-C16)
Cys_{353} - Cys_{358}	(C17-C18)

Example 3   Expression and purification of sHek subdomains

A series of sHek-derived cDNA constructs, designated sHek I-VII, encoding N-terminal FLAG™-tagged portions of the receptor exodomain according to the exon structure outlined above, is illustrated in Figure 1b. These constructs were transiently transfected into COS 7 cells, and the resulting culture supernatants were screened by immunodetection with anti-FLAG™ MAb for the production of recombinant proteins. Constructs yielding proteins of the expected size in culture supernatants were stably transfected into CHO cells. Appreciable expression levels were found for receptor-derived proteins, denoted sHek I-VII (exons 1-7), sHek I-VI (exons 1-4), sHek I-III (exons 1-3), sHek IV-VII (exons 4-7), and sHek V-VII (exons 5-7). Western blot analysis of the expressed proteins revealed the expected apparent molecular sizes for sHek I-VII (68k), sHek I-IV (36k), sHek I-III (33k), sHek IV-VII (40k), and sHek V-VII (36 k). Interestingly, no expression was observed for any of the protein constructs containing the exon 3-encoded domain, but missing the first

31 amino acids of sHek (encoded by exons 1 and 2), suggesting impaired transcription, translation or stability of these constructs.

Purification of sHek I-VII, sHek I-IV, sHek I-III and
5   sHek IV-VII by anti-FLAG™ MAb-affinity chromatography followed by anion exchange HPLC (sHek I-VII and sHek I-IV) or SE-HPLC (sHek I-III and sHek IV-VII) yielded homogenous preparations, as shown in Figure 1b, which were suitable for analysis of their interactions with LERK7 on the BIAcore™.
10

Example 4   Binding of various LERK-Fc fusion proteins to
                sensorchip-immobilised sHek

Receptor-ligand interactions within the EPH-type RTK family have been studied mainly by a modified indirect
15   Scatchard analysis of human IgG-Fc fusion proteins of ligands or receptors binding to receptor or ligand transfected cells, respectively (Beckmann *et al*, 1994; Davis *et al*, 1994; Ceretti *et al*, 1995; Bennett *et al*, 1995). To evaluate if BIAcore™ analysis also detected the interaction of various
20   LERKs with Hek, we compared the binding of bivalent, F_c-fusion proteins of LERK (1 to 5) and AL1/LERK 7 (Figure 2C) to sensor chip-immobilised sHek. Each ligand construct was injected at concentrations between 0.1-10 µg/ml (approximately 0.8 to 80 nM) across the sensor chip. A
25   sample containing 10 µg/ml of the recombinant human F_c fragment was used as a control. The relative binding response units (RU) of various samples at 10 µg/ml are illustrated in Figure 3, indicating comparable responses for LERKs 3, 4, 5 and 7 which were considerably greater than the responses of
30   LERK1 and LERK2. Apparent dissociation constants derived from equilibrium responses (equation 4) at the four highest concentrations suggested a decreasing order of nanomolar affinities, as follows:

AL1/LERK7 > LERK3 > LERK4 >> LERK5 (data not shown).

The interactions with LERKs 1 and 2 did not reach equilibrium responses in our experiments, and hence precluded estimation of dissociation constants. Only background binding was seen with the control recombinant F_C construct alone.

Example 5   Interaction kinetics of LERK3-FLAG™ and LERK7-FLAG™ binding to sHek

To evaluate the contribution of bivalency of F_c-ligand constructs to the interaction kinetics, we performed binding experiments with monovalent forms of LERK3 and LERK7. Corresponding FLAG™ peptide-tagged fusion proteins were expressed in CHO cells and purified to homogeneity from culture supernatants of selected clones by anti-FLAG™ affinity chromatography and ion exchange HPLC. The identity of the recombinant ligand proteins was confirmed by N-terminal amino acid sequence analysis.

A qualitative comparison of the BIAcore data, illustrating binding of increasing amounts of LERK 3-FLAG™ (Figure 4A) and LERK 7-FLAG™ (Figure 4B) to a Hek sensor chip, reveals marked differences in the kinetics of the two interactions. The LERK3/sHek interaction is characterized by extremely fast on and off rates, and comparable responses of LERK3 or LERK7-binding to sHek were found only at approximately 30-fold higher LERK3 concentrations in the applied sample. Kinetic analysis of the association and dissociation phases using a single component model yielded apparent association and dissociation rate constants of $k_a = 4.8 \pm 0.13 \times 10^5$ $M^{-1}s^{-1}$ and $k_d = 6.1 \pm 0.8 \times 10^{-3}s^{-1}$ for LERK7, and of $k_a = 3.7 \pm 0.9 \times 10^5 M^{-1}s^{-1}$ and $k_d = 0.26 \pm 0.06$ s^{-1} for LERK3. Apparent dissociation constants $K_D = 1.2 \times 10^{-8}$ M for LERK 7-FLAG™ and $K_D = 5.9 (\pm 0.4) \times 10^{-7}$ M for LERK 3-FLAG™

were estimated. Analysis of the raw data revealed good fits
to linear, "one-to-one" interactions, yielding Chi^2-values of
0.64 ± 0.18 and 0.47 ± 0.06 for the LERK7 and LERK 3
reactions, respectively. The apparent equilibrium affinity

5 constant for LERK7 was substantiated by Scatchard analysis of
the 'in-solution' interaction (Ward *et al*, 1995), yielding an
identical dissociation constant of $K_D = 1.2 \times 10^{-8}M$ (Figure
7C). On the other hand, the affinity of the LERK3/FLAG™
interaction was too low to obtain reliable data by "in-

10 solution" analysis.

*Cross linking of LERK-FLAG™ Proteins with anti FLAG™ Mab
alters interaction with sHek.*
We next addressed the possibility that the

15 differences observed in the binding of either FLAG™-tagged
and F_c-tagged ligands to sensorchip-immobilised sHek were due
to increased avidity of the divalent F_c tagged ligands. To
quantitatively examine this effect *in situ*, we assembled
bivalent ligand/Mab complexes before or during BIAcore

20 experiments by cross-linking FLAG™-tagged LERK7 (Figure 5A,
5B) and LERK-3 (Figure 5C, 5D) with the anti-FLAG™ Mab, M2.
The interactions of pre-formed LERK-FLAG™/M2 Mab
complexes (Figure 5B, 5D, graph e) with a sHek sensor chip
resulted in 3- to 5-fold increased BIAcore responses and

25 markedly reduced off-rates of the ligand/antibody complexes
compared to the non-complexed LERK-FLAG™ proteins (Figure 5A,
5C, graph c), reflecting the increased size, and indicating
an altered avidity, of the interacting complexes. To confirm
this, we injected FLAG™ peptide, competing with the LERK-

30 FLAG™ proteins for M2 Mab binding sites, into the
dissociation phase of LERK-FLAG™/M2 Mab complex (Figure 5B,
graph f, "↓ 2"). A dramatically increased off-rate in this
experiment confirmed that the suggested increase in avidity
was dependent upon M2 Mab-mediated cross linking of the LERK-

FLAG™ proteins. Furthermore, injection of the M2 Mab into dissociating LERK-FLAG™ proteins at the end of the first injection cycle ("↓ 2") resulted in a pronounced rise of the BIAcore signals, likely due to binding of newly-formed

5   ligand/Mab complexes (Figure 5B, 5D, graph d). The increase of the responses above the levels observed with the monovalent ligands in the first part of the sensorgram (between "↓ 1" and "↓ 2"), presumably reflects the increased size of the interacting ligand/Mab complexes. On the other

10   hand, amplitude and slope of the response curve are also determined by the abundance and affinity of the ligand available for complex formation at the time of Mab injection. Since injection of equimolar amounts of LERK3-Fc or LERK7-Fc are expected to yield the same ligand concentrations at the

15   end of the first injection cycles, differences in the amplitude of the response following Mab injection "↓ 2" (compare graph d in Figure 5B, 5D) must portray primarily the different affinities of the LERK-FLAG™/M2 Mab complexes. In support of this, the dissociation curves and the response

20   levels of pre-formed (graph e) and *in situ* formed (graph d) ligand/Mab complexes at the end of the second injection cycle (after 1090 s) were found to be identical (Fig 8D) or very similar (Figure 5B).

Taken together, this strictly qualitative analysis

25   demonstrates that M2 Mab-cross linked LERK-FLAG™ dimers bind sHek with increased avidity due to decreased dissociation rates. The resulting response curves are qualitatively very similar to the sensorgrams of the corresponding LERK-Fc fusion proteins, suggesting that avidity plays a major role

30   in the interaction kinetics of these ligand constructs.

Example 6   Induction of Hek phosphorylation in ligand-
              treated cell cultures

　　　In addition to the kinetic analysis of the LERK-sHek
interaction, we compared the ability of either LERK 3 or LERK
5   7 to mediate transphosphorylation of Hek in LK63 cells, which
have been shown to express the receptor constitutively (Boyd
et al, 1992).   LK63 cell cultures were incubated with buffer
or solutions containing either LERK 3-FLAG™, LERK 7-FLAG™ or
pre-formed complexes of these ligands with anti-FLAG™ Mab,
10   M2.   In the latter samples the concentrations of LERK-FLAG™
proteins and M2 Mab were adjusted to provide divalent ligand
constructs by accupancy of both binding domains of the Mab
with ligand-FLAG™ construct.   The Hek receptor was then
immunoprecipitated from the cells and analysed by western
15   blot analysis.   The results in Figure 6 illustrate the
analysis with PY20 anti-phosphotyrosine antibody (panel A)
followed by re-probing the stripped blots with rabbit anti-
Hek antibody.   Phosphotyrosine analysis shows no significant
differences between control (lane 5), LERK-3-FLAG™ (lane 4)
20   or LERK-7-FLAG™ (lane 3) treated samples.   In contrast,
incubation of cells with LERK-3-FLAG™/M2 complex induced a
small but significant increase (lane 2), and incubation with
LERK-7-FLAG™/M2 complex (lane 1) gave a dramatic increase in
phosphotyrosine content of Hek.   Corresponding bands on the
25   rabbit anti-Hek probed blots (panel B) show on significant
difference in total Hek protein between the experimental
groups.

Example 7   BIAcore™ analysis reveals the exon 3- encoded
30   Cys-rich region of sHek as the LERK 7 binding
              domain
　　　The interactions between EPH-like receptors and their
ligands have commonly been analysed by an indirect Scatchard
analysis of divalent receptor-exodomain/IgG1 fusion proteins

binding to ligand-expressing cells revealing equilibrium dissociation constants in the low nanomolar range (Winslow, 1995; Beckmann *et al*, 1994; Davis *et al*, 1994; Gale *et al*, 1996). In all these previous studies, the contribution of

5 the avidity of the bivalent Fc-fusion proteins has not been appreciated. In contrast, we have found an estimated K_d of 12 nM for the binding of LERK7 to BIAcore™ sensor chip-immobilised, monovalent sHek.

To evaluate the contribution of the various sHek

10 subdomains to the receptor/ligand interaction, we followed a similar strategy and performed a kinetic BIAcore™ analysis on the binding of sHek I-VII, I-IV, I-III and sHek IV-VII to sensor chip-immobilised LERK7. Deconvolution of the BIAcore™ raw data during the association and dissociation phases and

15 Scatchard analysis of the equilibrium responses (Biosensor, 1995) demonstrated monovalent, linear receptor/ligand interactions. Substantially lower dissociation constants (*ie*. higher affinities) of 18-29 nM, due to increased association rate constants (Figure 1D), were observed for the

20 interaction between LERK7 and the sHek subdomain constructs sHek I-IV and sHek I-III (Figure 1E). On the other hand, the very similar apparent dissociation constants of 72±15 and 62±12 nM for sHek and FLAG™-tagged sHek I respectively, and insignificantly higher equilibrium dissociation constants, as

25 shown in Figure 1E, suggested that an N-terminal addition of the FLAG™ peptide had no effect on the interaction between sHek and its ligand. Higher diffusion rates of the significantly smaller sHek subdomain constructs I-IV and I-III, and possibly an improved accessibility of the ligand

30 binding interface, are the most-likely reasons for the apparently increased affinity of these constructs observed in the BIAcore™ experiments.

Importantly, no binding of sHek IV-VII to immobilised LERK7 was observed at any of the concentrations

tested (16-500 nM), thus identifying the ligand binding site as lying within the N-terminal portion encoded by exon 1-3 of Hek. To evaluate the contribution of the most N-terminal 31 residues encoded by Hek exons 1 and 2, we performed in-

5 solution competition studies with a synthetic peptide, sHek$_{1-31}$, corresponding to this part of the receptor exodomain. The results, illustrated in Figure 2f, suggest that the presence of the 31-residue N-terminal peptide at concentrations up to 10 µM had no effect on the

10 receptor/ligand interaction, whereas addition of sHek I or sHek IV resulted in a dose-dependent reduction of the BIAcore™ response. Taken together these results unambiguously demonstrate that the cysteine-rich domain encoded by Hek exon 3 is the ligand binding domain.

15

Example 8   The effect of ectopic Hek expression in the developing zebrafish

Analysis of the Eph subfamily of RTKs and their ligands has centered largely on their role in axon guidance

20 (reviewed in Müller, et al, 1996; Friedman and O'Leary, 1996; Tessier-Lavigne, 1995), a process that occurs relatively late in embryogenesis. However, Eph receptors are expressed at much earlier stages in embryogenesis (Cheng and Flanagan, 1994; Henkemeyer, 1994; Xu et al, 1994; Gilardi-Hebenstreit,

25 1992; Nieto et al, 1992; Scales et al, 1995; Lickliter et al, 1996), and little is known about what role they might play at this stage. To address this role we have used the zebrafish, a model which has been previously shown to be tractable to analysis of early embryonic events (Xu et al, 1995, 1996).

30 These studies were remarkable because they demonstrated that ectopic expression of a mouse or Xenopus homologue of the zebrafish *rtk1* gene could be used to perturb development. Moreover, the effects were specific to the targeted gene in that defects were confined to regions of the zebrafish embryo

that expressed endogenous *rtk1*. The putative zebrafish Hek homologue, *rtk2*, is expressed during gastrulation from 80 to 90% epiboly in the dorsal axis and in a ring around the yolk plug. As epiboly completes, higher expression levels are

5 seen in the anterior neuraxis and in lateral cells of the neural plate aligned approximately with the mes-met boundary (XU *et al,* 1994). This localisation is similar to the patterns of the MEK4 transcript in the mouse embryo, which are seen at day 8.5 (10 somites) and show high levels of

10 expression at day 9.5 in the mid and hindbrain and within the paraxial mesoderm of the somites (Cheng and Flanagan, 1994).

We reasoned that ectopic sHek exodomain expression may cause defects in the brain development and somite organisation. Also, a high-affinity, 1:1 interaction between

15 the Hek exodomain and monovalent sLERK7 has been characterised and the need for ligand crosslinking (Figure 6) or cell association (Wilson *et al*, 1995) for receptor activation suggestws that both, receptor exodeomain and soluble ligand could serve as antagonists of signalling via

20 the zebrafish Hek-homologue.

We reasoned that ectopic sHek exodomain expression may cause defects in the brain formation and somite of the zebrafish embryo. Therefore, we tested the effect of a soluble, secreted form of the Hek receptor and of the ligand

25 LERK7 on zebrafish development. We compared this effect with a mutant Hek lacking the exon3-encoded LERK-7 binding domain identified in Example 7. A soluble form of the mouse Hek homolog, MEK4, has been isolated from an embryonic cDNA library (Sejjadi *et al*, 1991), suggesting that the early

30 mouse embryo is exposed to this form of the Hek protein. mRNA encoding the full length of a soluble form of the Hek extracellular domain, denoted sHek-I-VII-RNA or encoding sLERK7-FLAG™ (sLERK7-RNA), was introduced into zebrafish embryos at the single, two and four cell stages by

microinjection into the yolk cell immediately under the blastoderm. RNA introduced at this stage becomes ubiquitously distributed throughout the embryo (Figure 9d). We detected the presence of a FLAG™ epitope-containing

5 protein corresponding to the expected molecular weight for sHek-RNA in embryos from 5 hpf until 10hpf (Figure 9a), at an apparent concentration of 0.5 - 1 ng/embryo, demonstrating that the protein was present in embryos throughout the period of development analysed here.

10

Example 9 <u>Injection of full length sHek mRNA causes</u> <u>patterning defects in early embryogenesis</u>

Animals injected with sHek-RNA or sLERK7 RNA developed a consistent syndrome in a concentration dependent

15 manner. Inspection of the animals between 11 and 15 hours post fertilisation (hpf) revealed defects involving reduced dorsal axis height from the yolk cell, disorganised anterior neuraxis, and disorganised somite boundaries (Figure 7a-7f).

In severe cases of the syndrome at 12hpf (Figure 7b,

20 7e) there was little morphological differentiation visible along the anterior-posterior aspect of the dorsal axis. Axial tissue was flattened over the yolk cell and somites were elongated laterally, much as in the *trilobite* mutant (Hammerschmidt *et al*, 1996, Kane *et al*, 1996, Solnica-Krezel

25 *et al*, 1996, Stemple *et al*, 1996), and disorganised, often out of register across the dorsal midline. The anterior neuraxis was also disorganised so that optic vesicle formation was retarded, and the characteristic mid- and hindbrain segmentation visible at 13hpf was reduced or absent

30 (Figures 7b, 7e, 7c, 7f).

In less severely affected embryos, the defects were predominantly confined to the anterior portion of the dorsal axis.

Example 10   Analysis of marker gene expression

In order to better understand the nature of the
defect and to allow a more objective quantitation of the
proportion of embryos displaying defects, embryos injected
5   with sHek-RNA and sLERK7 RNA at three different mRNA
concentrations (100pg, 10pg and 1pg per embryo) were fixed
between 12 and 13hpf, and marker gene expression was
analysed. Animals were considered defective if *in situ*
hybridisation with probes to *hlx-1* (Fjose, 1994), *paxb*
10   (Krauss, 1991), *krox20* (Oxtoby and Jowett, 1993), and *myoD*
(Weinberg *et al*, 1994) revealed abnormal patterns consistent
with ectopic, gene expression. A dose-dependent effect of
sHek-RNA was seen across three orders of magnitude of mRNA
concentration (Figure 10a). The nature of these defects is
15   consistent with the gross morphological observations (Figure
8a, 8b) presented above. The most profound defect compared
with normal, uninjected embryos, is a failure of the mid, and
hind brain and trunk paraxial mesoderm to fuse across the
dorsal midline (Figure 8c-8f). The forebrain region was
20   intact, as indicated by a single axially-located stripe of
hlx-1 expression in the ventral forebrain. Cells expressing
paxb and *krox20* of the mid-and hindbrain respectively are
arrayed in lateral stripes at some distance from the dorsal
midline. Non-injected control embryos, or embryos injected
25   with E-GFP alone, do not show this defect (Figures 8a, 8b).
Thus a large gap separating left and right halves of the
embryo is present from the posterior limit of the forebrain
until the anterior level of the somites. This analysis
suggests that there has been a failure of the cells of the
30   mid-and hindbrain to converge to the dorsal axis correctly.
Disorganised *myoD* expression confirms (Figure 8d, 8f) the
observation in living embryos that many somites are out of
register across the midline. This defect could result from a
failure of lateral cells to converge to the midline, a

conclusion consistent with the laterally-extended somitic
segmentation seen in live embryos. However, an disruption of
anterior-posterior patterning processes cannot be ruled out.
A coherence of phenotypes in response to exogenous expression
5   of either receptor exodomain or soluble ligand indicate
specific rather than promiscuous activation of the endogenous
Hek homologue by a putative zebrafish homologue of LERK7.

We verified this notion by markedly reducing the
number of defective embryos by co-injecting Hek-RNA together
10   with LERK7-RNA (Figure 10a). Importantly, our experiments
confirm a strict conservation of structural and functional
specificity of Eph-like receptors in vertebrate development.

Example 11   Deletion of the ligand binding domain from the
15   sHek-FL mRNA rescues embryonic development
The assignment *in vitro* of the domain in Hek that is
responsible for high affinity binding to LERK-7 by methods as
described in Example 4, was tested *in vivo* by introduction of
a mutated version of sHek into zebrafish embryos. We have
20   shown in Figure 1d and e that the extracellular domain of the
Hek receptor requires the presence of the sequence encoded by
exon 3 in order to show high affinity binding to LERK-7.
This assignment provides that removal of exon 3 from the sHek
mRNA injected into zebrafish embryos should abrogate all
25   developmental defects due to the interaction of Hek with
ligand through this domain. Therefore, the corresponding
mRNA, sHek-IV-VII-RNA, was injected into zebrafish embryos at
the same range of concentrations at which the full-length
sHek-RNA had produced defective development. The resulting
30   embryos were assayed and scored for disrupted marker gene
expression patterns as described above.

No significant developmental defects were detected in
embryos injected with either 10pg or 1pg per embryo sHek-IV-
VII-RNA, either by gross morphological criteria (Figure 9c),

or by analysis of marker gene expression (Figure 9g).
Ubiquitous E-GFP expression (Figure 9d) and detection of
approximately 0.4 - 1.0 ng sHek IX protein per embryo by
Western blotting (Figure 9a) during development indicate that
5   the protein was widely and highly expressed. Thus the
failure of cells to converge to the dorsal midline in embryos
injected with sHek-RNA is a function of the exon 3-encoded
ligand binding domain, and is probably due to interaction of
this domain with one or more LERK-like ligands present in the
10   embryo. Interestingly, at high concentrations (100 pg per
embryo) of injected sHek-IV-VII-RNA, there was no difference
in the proportion of defective embryos when compared to sHek-
RNA injected embryos. This indicates that at high
concentrations of receptor extracellular domain, the
15   developmental perturbation becomes effectively ligand
independent and indicates a distinct receptor dimerisation
interface within the exon 4-7 encoded subdomains.

DISCUSSION
20   Most of the studies of EPH-like receptors and their
ligands carried out to date have been performed with divalent
(F_c fusion) constructs of either ligand or receptor. We
compared the binding of differenct LERK-F_c fusion proteins to
Hek sensor chips, and confirmed the suggested cross-
25   reactivity of all the tested LERK-F_c constructs with Hek
(Fig. 4). In accord with these reports, the interaction
between Hek and F_c constructs of LERKs 1 and 2 was
distinctively weaker than binding of LERKs 3 and 4, which in
our experiments yielded similar BIAcore responses to LERK 7.
30   On the other hand, while the previously published affinities
of LERKs 1, 2 and LERK 5-F_c for Hek are very similar (18, 43,
and 23 nM, respectively, (Beckmann *et al*, 1994; Cerretti *et
al*, 1995), we could estimate apparent dissociation constants
only from equilibrium responses of LERKs 3,4,5 and LERK7-F_c

(K_Ds of 5, 6, 24 and 3 nM, respectively), whereas binding of LERKs 1 and 2 was too weak for a kinetic analysis. In addition, biphasic binding was reported previously only for the interaction between Hek-F_c with LERK 2, where a low

5   affinity constant of 430 nM was found (Beckmann *et al*, 1994). Our comparative analysis of the association and dissociation phases of two candidate Hek ligands, LERK3 (Kozlosky *et al*, 1995) and LERK7 (Lackmann *et al*, 1996) indicated a concentration-dependent increase of the apparent dissociation

10   rate constants (not shown) and an increasingly poor fit to the assumed one-component dissociation model (Table 3).

A significant deviation of the divalent LERK-Fc kinetics from linear, single component interactions, suggesting a high-affinity interaction at low and a low-

15   affinity interaction at high ligand concentrations confirms earlier studies by Hogg *et al*, 1987, and Posner *et al*, 1991, which demonstrate that kinetic models based on a one-to-one stoichiometry do not adequately describe the dissociation of bivalent solutes from surface-bound receptors.

20   The use of different approaches for the kinetic analysis of Hek/LERK-Fc interactions could explain the differences between the published data and our findings. A direct evaluation of kinetic data from BIAcore progress curves in likely to be more sensitive to changes in kinetic

25   rate constants than "indirect Scatchard analysis" which relies on the use of labelled mouse anti-human IgG antibodies to detect receptor-Fc fusion proteins bound to ligand-transfected cells (see for example Davis *et al*, 1994; Beckman *et al*, 1994). Competitive binding experiments of the LERK-Fc

30   /Hek interaction in solution (Figure 6) which are not affected by immobilisation artefacts and/or rebinding of dissociating ligand (Ward *et al*, 1995; Chatellier *et al*, 1996) but rely on an "indirect" estimation of bound ligand or receptor (see Methods), gave no direct indication of biphasic

kinetics from the slope of the Scatchard plots but yielded negative [^{B}LERK/^{F}LERK] values at low sHek concentrations, thus indicating artefactually high responses in these samples. The interaction of bivalent LERK7-F$_c$, containing only a

5 single bound sHek, via the remaining free LERK7 moiety to the sHek sensor surface, is a likely explanation for this artefact and confirms the concentration-dependent bivalency of the LERK-Fc/Hek interaction.

The comparative evaluation of all our binding data

10 suggests that the bivalent, high-affinity interaction of two covalently linked binding domains of the ligand/Fc fusion protein with two adjacent, sensorchip-immobilised receptor molecules will compete at saturating ligand/Fc concentrations with a low-affinity, monovalent interaction of a single

15 binding domain with a single receptor molecule. Similar effects have been described for the analysis of Mab/antigen interactions (see for example Chatellier *et al*, 1995) and for the interaction of dimeric interleukin (IL)6 with the sensorchip-immobilised IL6 receptor-exodomain (Ward *et al*,

20 1996).

In other studies of Eph receptor/LERK interactions the effect of solute bivalency has not been addressed. The necessity of ligand clustering for efficient receptor activation (Winslow *et al*, 1995; Davis *et al*, 1994; Cerretti

25 *et al*, 1995) seemed to warrant the use of bivalent receptor or ligand constructs. Such constructs were also used most recently in whole embryo *in situ* staining to confirm kinetic experiments performed with the same receptor-Fc constructs (Gale *et al*, 1996). On the other hand, it remains to be

30 demonstrated that the interaction between membrane-bound ligands (or receptors) and F$_C$-tethered, bivalent receptors (or ligands) is a suitable system to study kinetics of physiological interactions of membrane-bound ligands and receptors (Pandey *et al*, 1995). Our experiments indicate

that the artificial bivalency of the ligand constructs
obscures an unambiguous analysis of the reaction kinetics.
In agreement with a report on the kinetics of the cell
adhesion molecule CD 2 and its GPI-anchored ligand, CD 48
5   (van der Merwe *et al*, 1993) we find that very low affinity,
due to fast ligand dissociation, is apparently increased by
high avidity-binding of multimeric ligand aggregates.

By analysing the binding of monovalent LERKs to sHek,
either in solution (not shown) or using the (sensor) surface-
10   immobilised receptor (Figures 4, 5), we were able to
characterise the receptor/ligand interaction in detail. *In
situ*-crosslinking of the monovalent ligands with a MAb during
BIAcore experiments (Figure 5) and prior to SE-HPLC analysis
of LERK/sHek complexes (not shown) demonstrated qualitatively
15   the effect of avidity on the interaction and confirmed the
apparent higher affinities of bivalent ligand constructs.
Differences, in the dissociation phases of specific LERK
interactions were concealed by the higher avidity of divalent
binding components (Figure 5) but have a major impact on the
20   affinities of the monovalent ligands (Figures 4,5). Due to
an extremely fast off-rate, the interaction of monovalent
LERK3-FLAG™ with the immobilised receptor is very weak
(Figure 4B), an observation confirmed in solution which
indicated an unstable, transient LERK3-FLAG™/sHek complex.
25   By contrast, binding of LERK7-FLAG™ to sHek was characterised
by a 40-times lower off rate and resulted in a stable
receptor/ligand complex (not shown) which was confirmed by
kinetic analysis of sHek binding to sensor chip-immobilised
LERK7, yielding an apparent K_D of 7.2 x 10^{-8} M. The
30   dissociation rate of the LERK7-FLAG™/sHek reaction was low
enough to allow purification of the ligand/receptor complex
from solution and to facilitate its characterisation by
equilibrium sedimentation analysis. The demonstration of a
1:1 stoichiometry confirms our findings from BIAcore and SE-

HPLC experiments, indicating that Hek has a single binding site for LERK7, and explaining the necessity of ligand-crosslinking for receptor activation and trans-phosphorylation demonstrated in this study (Figure 6) and

5   reported by others (Davis *et al*, 1994; Brambilla *et al*, 1995).

Our results clearly identify LERK7 as the best candidate for a physiological Hek ligand. Despite very similar apparent affinity constants for the LERK-3 and LERK-7

10   F_C fusion proteins, the interaction between their monovalent analogues and sHek differs substantially by a markedly higher dissociation rate of LERK3-FLAG™ protein. Cross-linking of the dissociating ligands with anti-FLAG™ MAb decreases the dissociation rates and results in similar interaction

15   kinetics for both ligands. Our results could suggest, that the reported interactions between some of the LERKs and Hek are influenced by the choice of the ligand construct. Extrapolating our observations to the *in vivo* situation, it seems likely that LERK3 functions as an effective ligand only

20   at very high receptor and ligand densities on opposing cell membranes, whereas a stable LERK7/Hek complex persists at much lower receptor and ligand numbers.

SUMMARY

25   *Identification of the ligand binding domain mechanism of*
perturbation of vertebrate embryogenesis with soluble Hek
exodomain and soluble LERK7

Specialised roles during vertebrate development have been described for a limited number of Eph-receptors and the

30   corresponding ligands (Cheng et al., 1995, Drescher et al., 1995, Nakamoto et al., 1996) and together with the high interspecies conservation of primary protein structures argues for conserved and specific functions of defined Eph receptor/ligand interactions. A comparison between the amino

acid sequences for the extracellular domains of Hek and its
murine (MEK4) and chicken (CEK4) homologues (96 and 91%
overall identity, respectively) demonstrates highest identity
in the exon III encoded domain (99.5 % and 99.3%,

5   respectively, Fig. 1a) and suggests a high evolutionary
constraint on the structure of this domain. By analysing the
interactions of the receptor exodomain and derived subdomains
(Fig. 1b, c) with its high-affinity ligand *in vitro* by
BIAcore analysis and *in vivo* by expression in zebrafish, we

10   were able to confirm this notion. BIAcore experiments
summarised in Figures 1d, 1e, 1f demonstrate that the exon
III-encoded subdomain is both, sufficient and neccessary for
high-affinity ligand binding. Whereas expression of the Hek
exodomain or of soluble LERK 7 during zebrafish embryogenesis

15   results in dose-dependent disruption of midline development,
expression of the truncated receptor lacking the ligand
binding domain gives rise to unaffected embryos, emphasising
the role of a Hek/LERK7 derived signal during vertebrate
development. A partial rescue of the wildtype phenotype by

20   co-injection of receptor exodomain- and soluble LERK 7-mRNA
suppports the specificity of the observed effect for a Hek-
LERK 7 interaction.

        We assume that the sHek protein acts in a dominant
negative manner in the embryo. Previous studies in cell

25   culture and in embryos have demonstrated that signalling
through RTKs is inhibited by coexpression of kinase-deleted
or truncated forms of the receptor (Honegger *et al*, 1990;
Frattali *et al*, 1992a, b, Spritz *et al*, 1992; Reith *et al*,
1993; Peters *et al*, 1994, Dumont *et al*, 1994). This

30   inhibition is thought to proceed via the formation of a
dimeric complex on the surface of cells, in which an
endogenous full-length length receptor pairs with the
exogenous truncated receptor, resulting in a complex that
cannot transphosphorylate, and hence is inactive in signaling

(reviewed in Van der Geer et al., 1994). The formation of these complexes can be either ligand dependent (Ueno et al., 1993) or independent (Frattali et al., 1992a,b, Levi-Toledano, 1994). Expression of a kinase domain-deficient Eph

5   subfamily receptor has been used previously to disrupt the signaling of *rtk1*/sek1 in zebrafish embryos (Xu et al., 1996).

We interpret the results described here using a model in which the secreted Hek extracellular domain bind or

10 secreted sLERK7 to an endogenous receptor-ligand multimer and render this complex inactive. These soluble forms can also bind ligand (receptor) independently of the endogenous receptor (ligand), as demonstrated by our results *in vitro* (Figure 11g, 11e), thereby titrating the ligand (receptor)

15 from the system. Both molecular mechanisms have the same effect: a decrease in the number of active cell surface receptor-ligand signaling complexes. Recent results indicate that transmembrane Eph receptor ligands may have the capacity to transduce a signal into the cells on which they are

20 expressed (Holland et al., 1996, Bruckner et al., 1997). However, as LERK7 is GPI-linked to the cell surface, ligation to the Hek receptor is not expected to generate a signal in this manner.

25   It will be apparent to the person skilled in the art that while the invention has been described in some detail for the purposes of clarity and understanding, various modifications and alterations to the embodiments and methods described herein may be made without departing from the scope

30 of the inventive concept disclosed in this specification.

References cited herein are listed on the following pages, and are incorporated herein by this reference

REFERENCES

Anson, D.S. *et al.*
EMBO J., 1984 <u>3</u> 1053-1060

5

Beckmann, M.P. *et al.*
Embo Journal, 1994 <u>13</u> 3757-3762

Bell, G.I. *et al.*
10   Nucleic Acids Res., 1986 <u>14</u> 8427-8446

Biosensor, P.
BIAtechnology Handbook (Pharmacia Biosensor AB, Uppsala, Sweden, 1995).

15

Bonhoeffer, F. and Sanes, J.R.
Curr. Opin. Neurobiol., 1995 <u>5</u> 1-5

Brambilla, R. *et al.*
20   Embo Journal, 1995 <u>14</u> 3116-3126

Brennan, C. *et al.*
Development, 1997 <u>124</u> 655-664

25   Cerretti, D.P. *et al.*
Molecular Immunology, 1995 <u>32</u> 1197-1205

Cheng, H.J. and Flanagan, J.G.
Cell, 1994 <u>79</u> 157-168

30

Cheng, H.J., Nakamoto, M., Bergemann, A.D. and Flanagan, J.G.
Cell, 1995 <u>82</u> 371-381

Connor, R.J. and Pasquale, E.B.

Oncogene, 1995 11 2429-2438

Davis, S. *et al.*
Science, 1994 266 816-819

5

Drescher, U. *et al.*
Cell, 1995 82 359-370

Friedman, G.C. and O'Leary, D.D.
10 Current Opinion in Neurobiology, 1996 6 127-133

Gale, N.W. *et al.*
Neuron, 1996 17 9-19

15 Giger, R.J. *et al.*
Eur. J. Biochem., 1995 227 617-628

Gilardi-Hebenstreit, P. *et al.*
Oncogene, 1992 7 2499-2506
20

Green, J.B.A. and Smith, J.C.
Trends in Genetics, 1991 7 245-250

Henkemeyer, M. *et al.*
25 Oncogene, 1994 9 1001-1014

Kennedy, T.E. and Tessier-Lavigne, M.
Current Opinion in Neurobiology, 1995 5 83-90

30 Kozlosky, C.J. *et al.*
Oncogene, 1995 10 299-306

Lackmann, M. *et al.*
Proc Nat Acad Sci (USA), 1996 93 2523-7

Lickliter, J.D., Smith, F.M., Olsson, J.E., Mackwell, K.L. and Boyd, A.W.
Proceedings of the National Academy of Sciences of the United States of America, 1996 <u>93</u> 145-150

Maisonpierre, P.C., Barrezueta, N.X. and Yancopoulos, G.D.
Oncogene, 1993 <u>8</u> 3277-3288

Mount, S.M.
Nucleic Acids Res, 1982 <u>10</u> 459-472

Müller, B.K., Bonhoeffer, F. and Drescher, U.
Current Opinion in Genetics and Development, 1996 <u>6</u> 469-474

Nakamoto, M. *et al.*
Cell, 1996 <u>86</u> 755-766

Nieto, M.A.
Neuron, 1996 <u>17</u> 1039-1048

Nieto, M.A., Gilardi-Hebenstreit, P., Charnay, P. and Wilkinson, D.G.
Development, 1992 <u>116</u> 1137-1150

Oldberg, A. and Ruoslahti, E.
J. Biol. Chem., 1986 <u>261</u> 2113-2116

Pandey, A., Duan, H. and Dixit, V.M.
Journal of Biological Chemistry, 1995 <u>270</u> 19201-19204

Pandey, A., Lazar, D.F., Saltiel, A.R. and Dixit, V.M.
Journal of Biological Chemistry, 1994 <u>269</u> 30154-30157

Pandey, A., Lindberg, R.A. and Dixit, V.M.
Current Biology, 1995 5 986-989

Pawson, T. and Bernstein, A.
5 Trends Genet., 1990 6 350-356

Sajjadi, F.G., Pasquale, E.B. and Subramani, S.
New Biologist, 1991 3 769-778

10 Scales, J.B., Winning, R.S., Renaud, C.S., Shea, L.J. and
Sargent, T.D.
Oncogene, 1995 11, 1745-1752

Sudhof, T.C., Goldstein, J.L., Brown, M.S. and Russell, D.W.
15 Science, 1985 228 815-822

Tessier-Lavigne, M.
Cell, 1995 82 345-348

20 Tessier-Lavigne, M. *et al.*
Eph nomenclature (EMBL, Heidelberg, Germany, 1996).

Tuzi, N.L. and Gullick, W.J.
British Journal of Cancer, 1994 69 417-421
25

Wicks, I.P. *et al.*
Genomics, 1994 19 38-41

Winslow, J.W. *et al.*
30 Neuron, 1995 14 973-981

Xu, Q., Alldus, G., Holder, N. and Wilkinson, D.G.
Development, 1995 121 4005-4016

Xu, Q., Holder, N., Patient, R. and Wilson, S.W.
Development, 1994 <u>120</u> 287-299

LUDWIG INSTITUTE FOR CANCER RESEARCH

5   THE QUEENSLAND INSTITUTE OF MEDICAL RESEARCH

THE UNIVERSITY OF QUEENSLAND

THE LEUKAEMIA FOUNDATION OF QUEENSLAND

25 June 1997

A

I II III IV V VI VII

cys rich EGF-like FNIII FNII

B

| 65 | 96 | 99.5 | 91 | 94 | 95 | 94 | MEK4 |
| 50 | 86 | 99.3 | 91 | 89 | 88 | 89 | CEK4 |

HEK I

HEK III

HEK IV

HEK IX

C

M_r

66.3 —
55.4 —

36.5 —
31 —

sHEK sHEKI-VII sHEKIV-VII sHEKI-IV sHEKI-III

D

$K_a \times 10^5$ (M^{-1}s^{-1})

sHEK sHEKI-VII sHEKI-IV sHEKI-III sHEKIV-VII

E

K_d (nM)

sHEK sHEKI-VII sHEKI-IV sHEKI-III sHEKIV-VII

F

% of Total Response

Competitor Concentration [μM]

FIGURE 1

ML059701.cdr
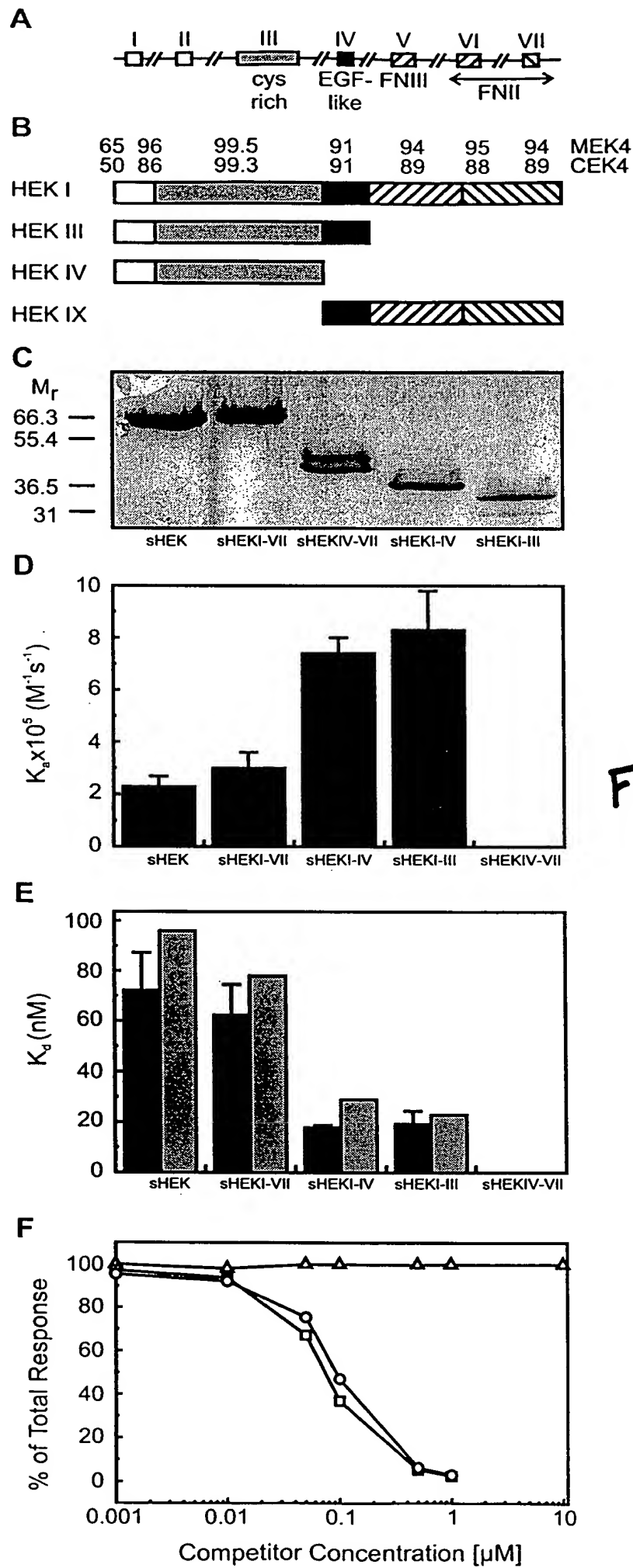
EXTRACELLULAR DOMAIN   HYDROPHOBIC TAIL

A.

GPI

B.

C.

S
S
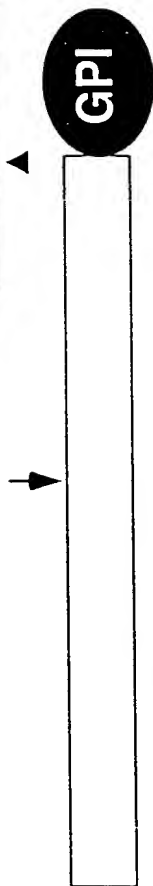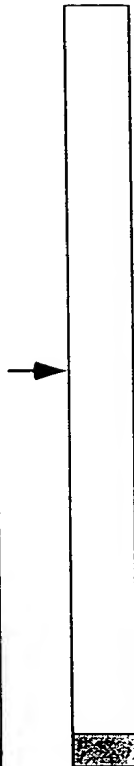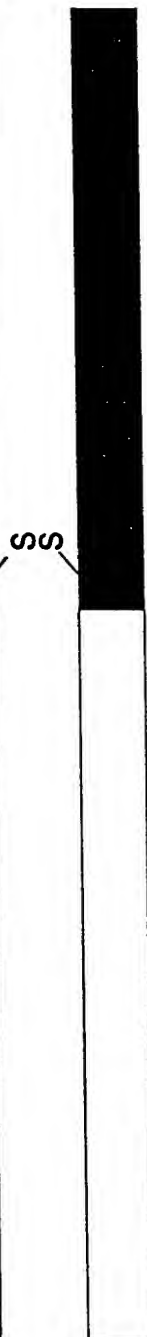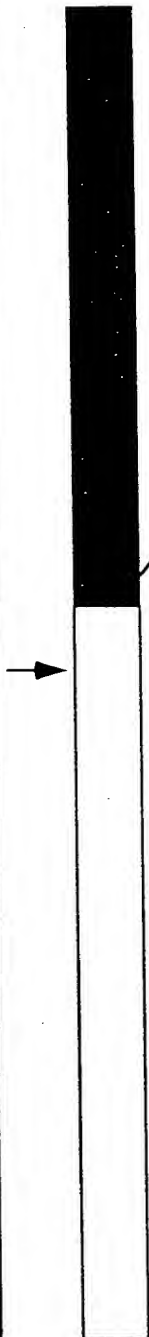
LERK7 SIGNAL
SEQUENCE

IL-3 SIGNAL
SEQUENCE

FLAG™
SEQUENCE

FIGURE 2
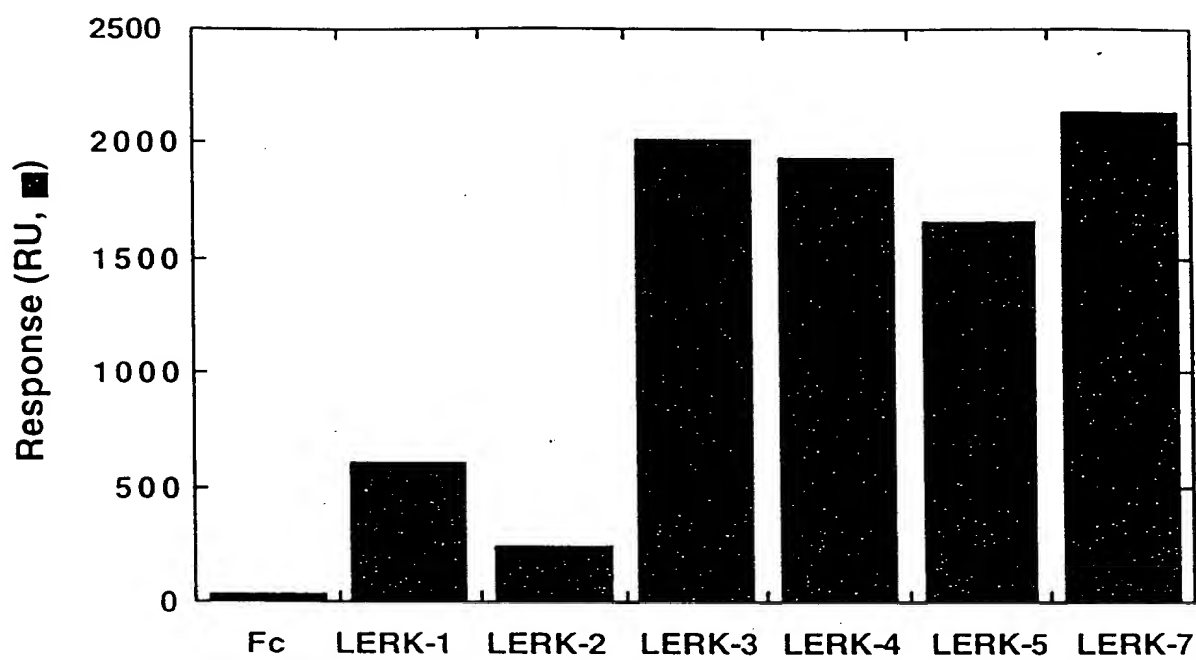
FIGURE 3
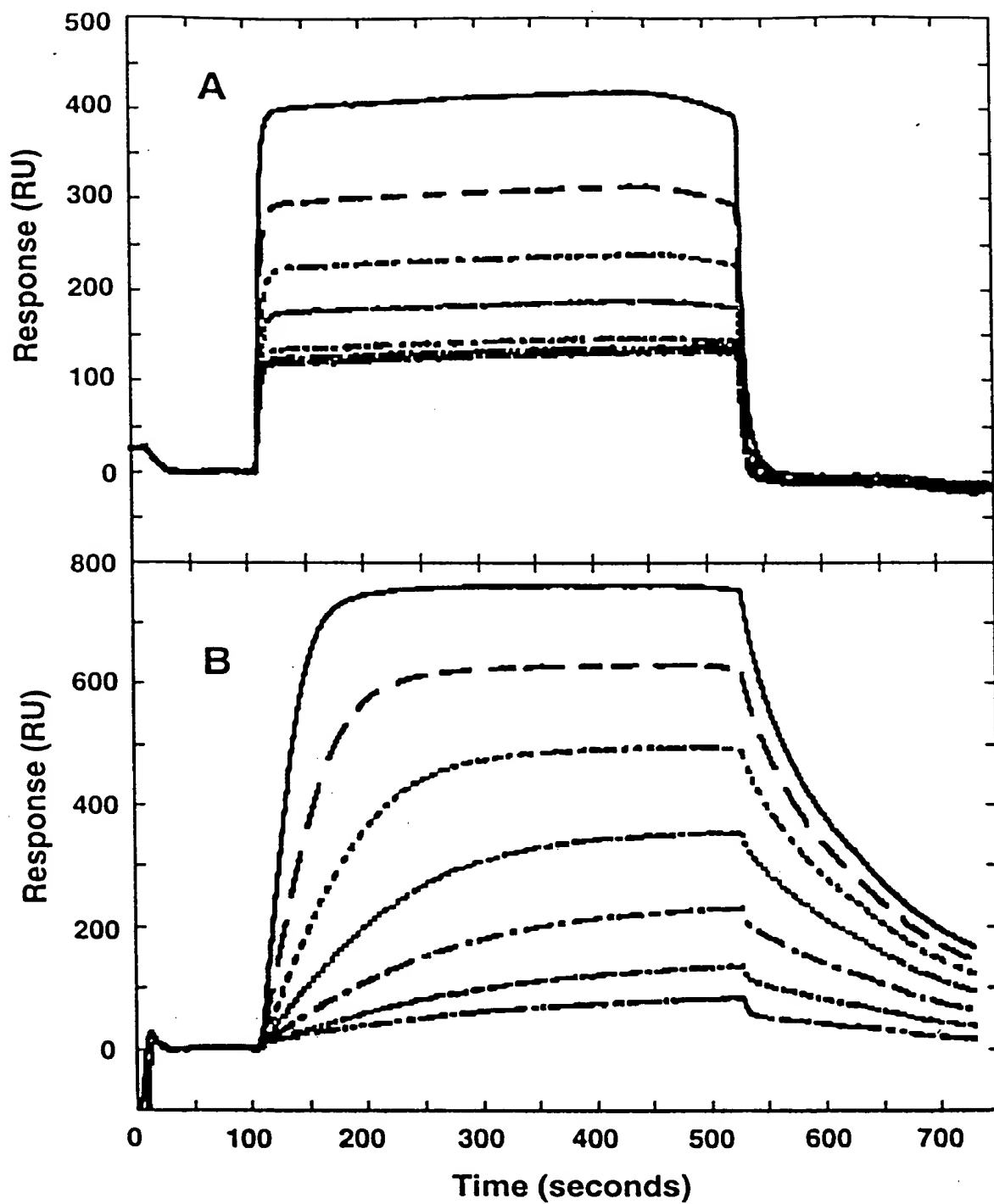
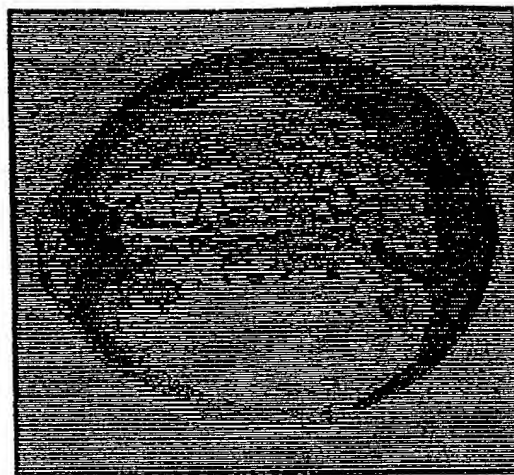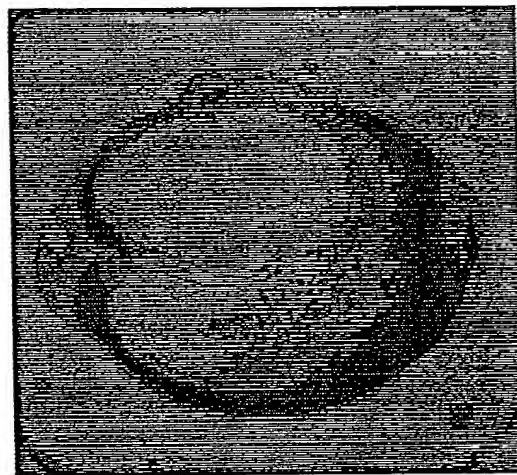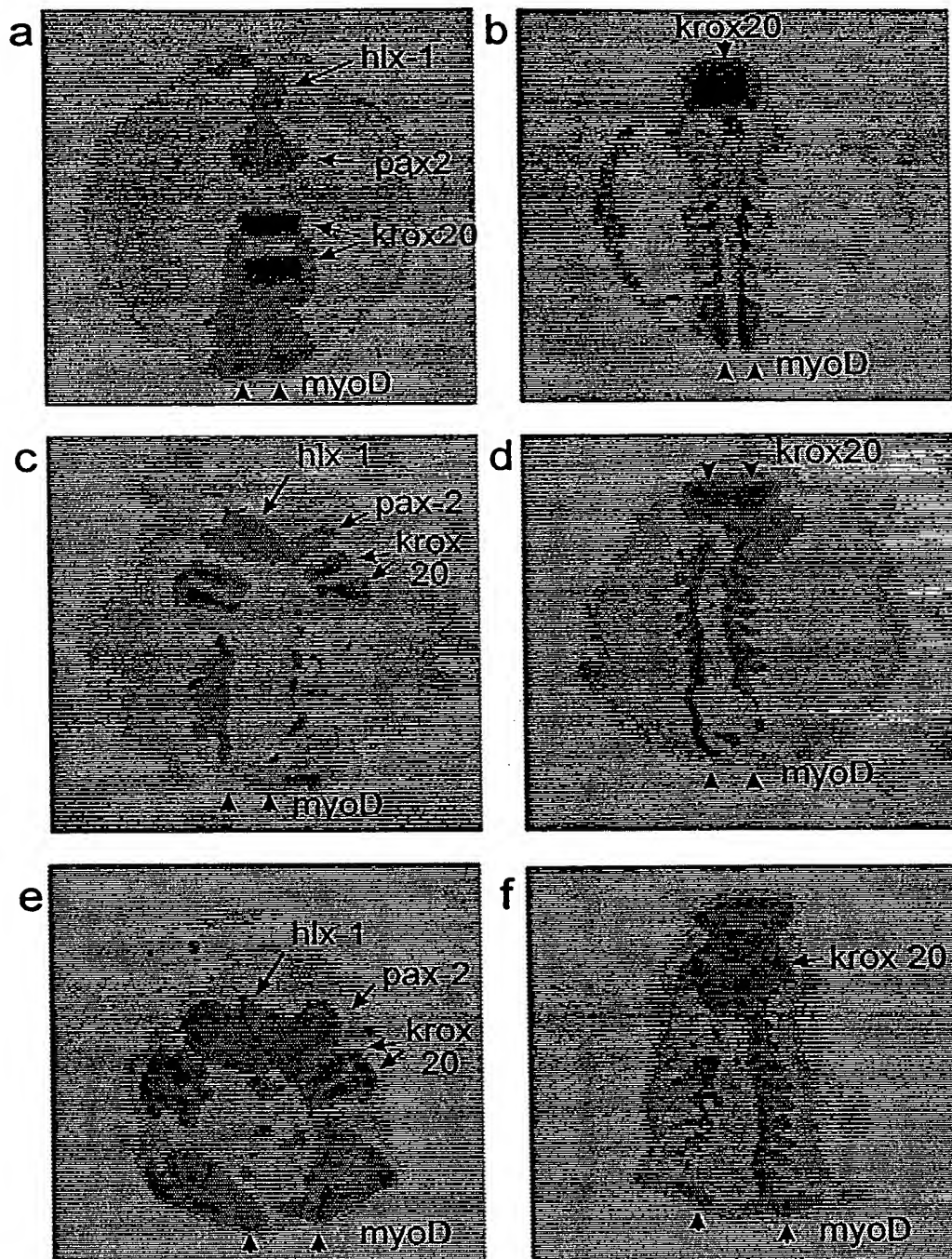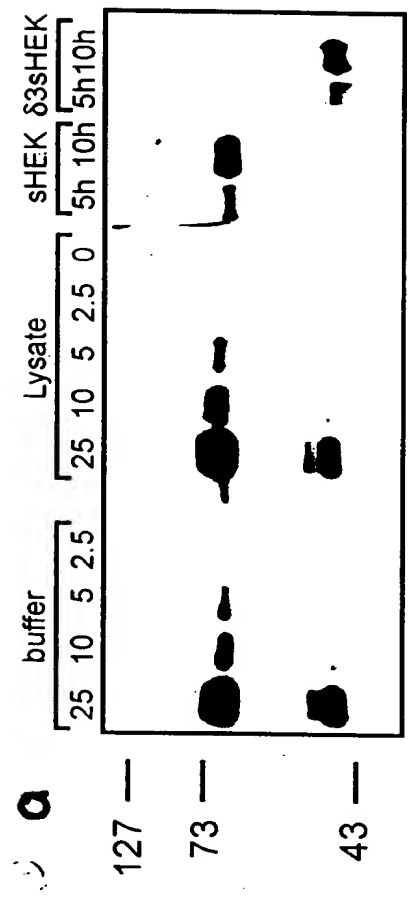FIGURES 4a to 4b

FIGURE 4c

Response (RU)
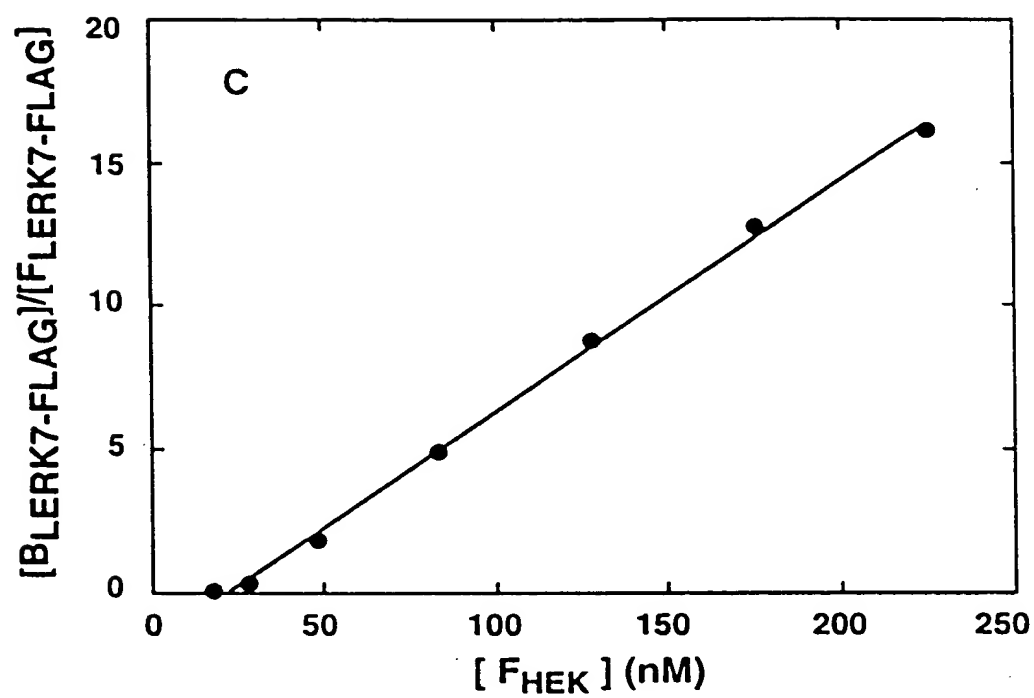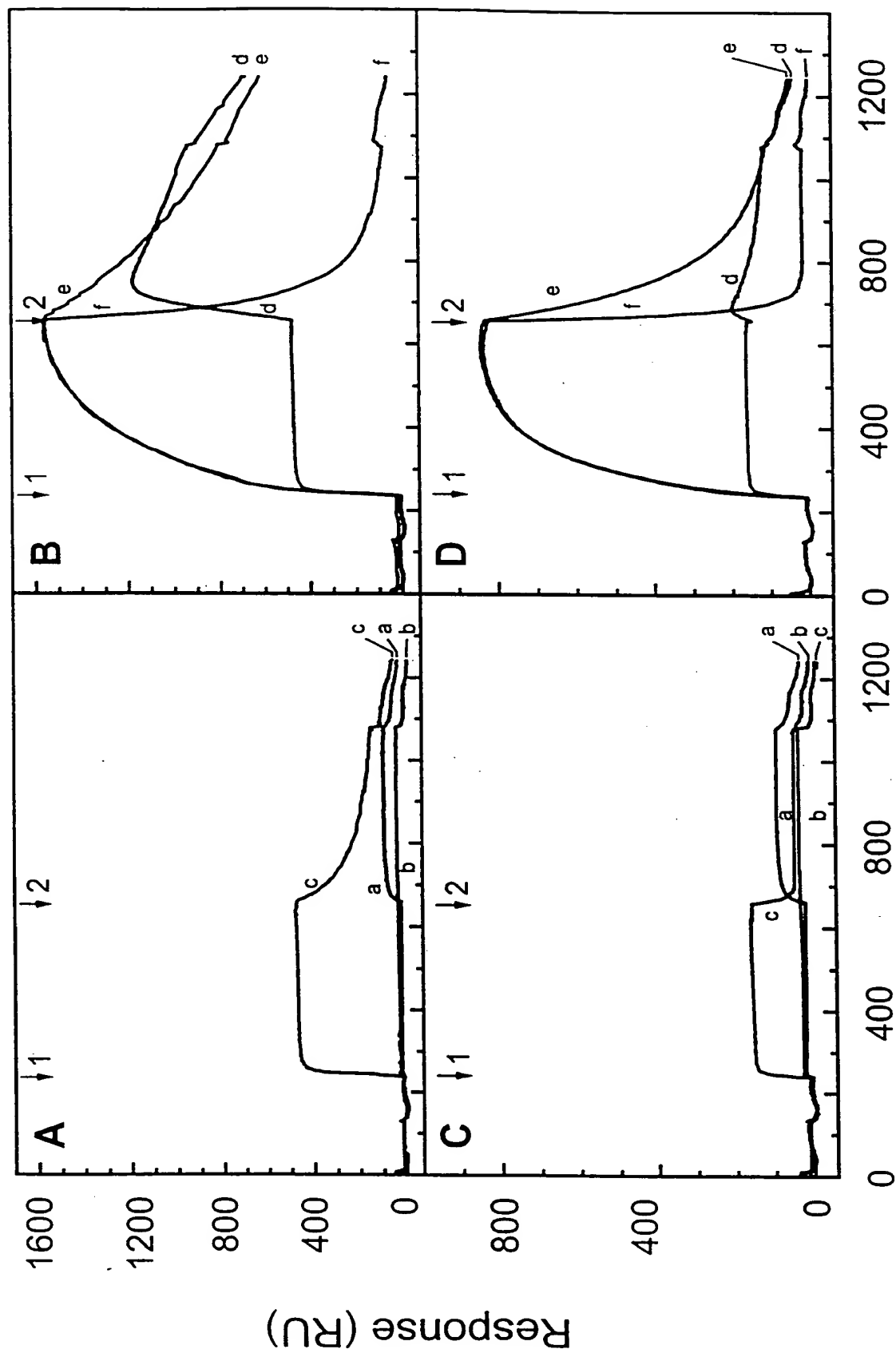
Time
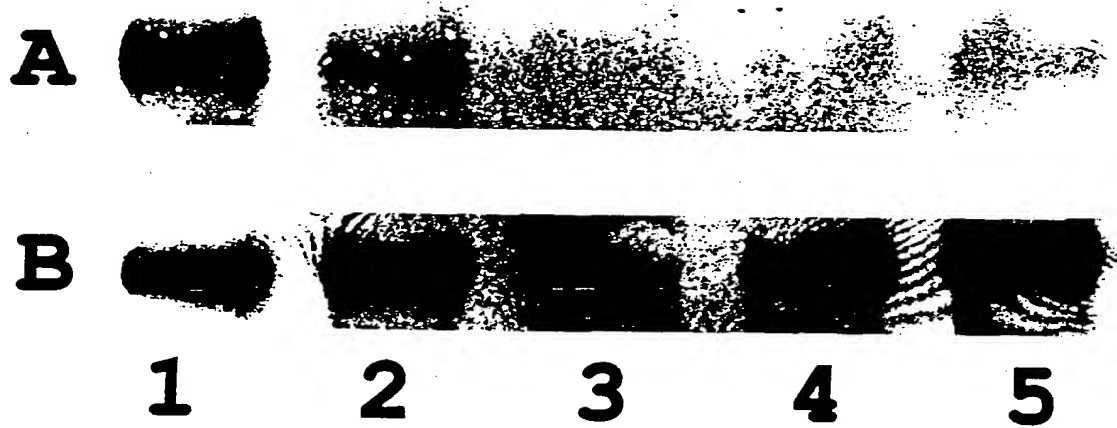
FIGURE 5

FIGURE 6
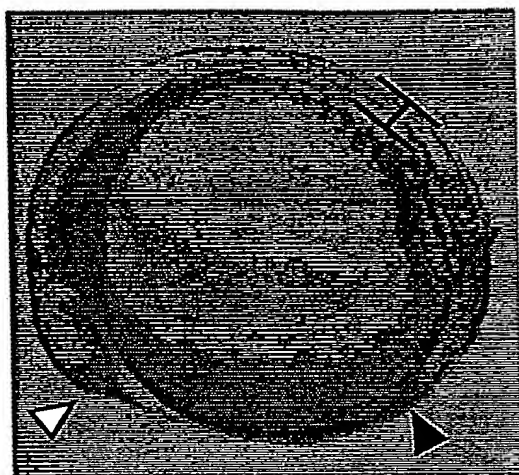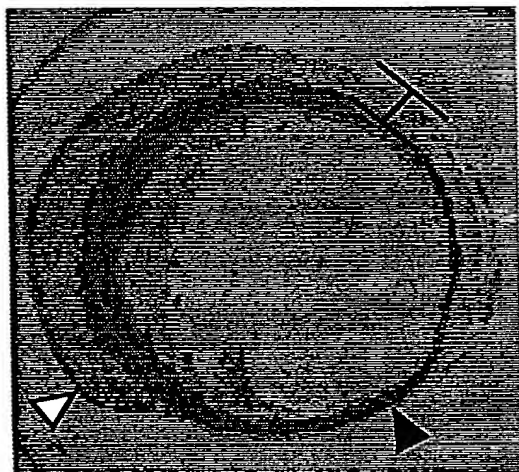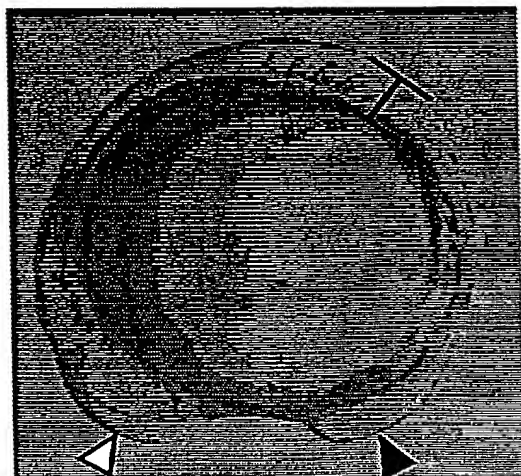
FIGURE 7

a069701.cdr

FIGURE 8

FIGURE 9a

FIGURES 9b to 9g